RESEARCH ARTICLE SUMMARY

BLOOD STEM CELLS

Retrotransposons are co-opted to activate hematopoietic stem cells and erythropoiesis

Julia Phan, Brandon Chen, Zhiyu Zhao, Gabriele Allies, Antonella Iannaccone, Animesh Paul, Feyza Cansiz, Alberto Spina, Anna-Sophia Leven, Alexandra Gellhaus, Dirk Schadendorf, Rainer Kimmig, Marcel Mettlen, Alpaslan Tasdogan*, Sean J. Morrison*

INTRODUCTION: Under steady-state conditions in adult mammals, hematopoietic stem cells (HSCs) reside in a quiescent state within the bone marrow. However, during hematopoietic stresses, HSCs are activated to increase the production of blood cells in extramedullary tissues, such as the spleen. For example, blood volume increases during pregnancy, necessitating increased red blood cell production to avoid maternal anemia. Consequently, HSCs and extramedullary erythropoiesis are activated during pregnancy to maintain red blood cell counts, though our understanding of the underlying mechanisms is limited. In this study, we explored these mechanisms in mice and humans.

RATIONALE: We performed RNA sequencing (RNA-seq) of HSCs isolated from pregnant and nonpregnant mice and humans as well as of HSCs after serial bleeding in mice to identify changes in gene expression that regulate HSC activation by these stresses. Although it is common to discard repetitive sequences during the processing of RNA-seq data, we elected not to do so. Repetitive sequences include retrotransposons, germline DNA elements that encode an enzyme that reverse transcribes retrotransposon transcripts into DNA, which can reinsert in other locations in the genome. Given that reinsertion can mutate genes, retrotransposon

transcription is repressed under normal circumstances. Nonetheless, DNA damage or changes in chromatin structure can promote the transcription of retrotransposons. Reverse transcription of retrotransposons leads to the activation of innate immune pathways, including cyclic guanosine 3′,5′-monophosphate–adenosine 5′-monophosphate synthase (cGAS) and stimulator of interferon (IFN) genes (STING), which induce IFN production and changes in the expression of IFN-regulated genes. Deficiency of cGAS or STING has little or no effect on HSCs or hematopoiesis under normal circumstances, consistent with retrotransposon repression in normal hematopoietic cells. In this study, we tested whether retrotransposons or cGAS-STING regulate changes in HSC function or hematopoiesis during pregnancy.

RESULTS: We found that retrotransposon transcription increased in mouse HSCs but not in most other hematopoietic cells during pregnancy and after serial bleeding. To test whether this contributed to HSC activation or erythropoiesis during pregnancy, we treated mice with reverse transcriptase inhibitors, which would prevent cGAS-STING activation by retrotransposons. Reverse transcriptase inhibitors had little effect on hematopoiesis in nonpregnant mice but reduced HSC cell division and the numbers of HSCs and erythroid

progenitors in the spleens of pregnant mice as well as red blood cell counts. STING or cGAS deficiency had little effect on hematopoiesis in nonpregnant mice but reduced HSC cell division and the numbers of HSCs and erythroid progenitors in the spleens of pregnant mice as well as red blood cell counts.

cGAS-STING signaling promotes IFN expression, leading to changes in IFN-regulated gene expression, and IFNs can promote HSC activation. HSCs from pregnant mice exhibited increased IFN expression and changes in IFN-regulated gene expression compared with HSCs from nonpregnant mice, and these changes were largely blocked by STING deficiency. Deficiency for the type 1 IFN receptor had little effect on hematopoiesis in nonpregnant mice but reduced the numbers of HSCs and erythroid progenitors in the spleens of pregnant mice. Together, these data suggest that after erythropoietic stresses, retrotransposon transcription increases in HSCs, leading to cGAS-STING activation and IFN expression, increasing HSC cell division and erythropoiesis. To test whether this occurs in humans, we isolated HSCs from the blood of pregnant and nonpregnant females. HSCs from most humans also exhibited increased retrotransposon transcription during pregnancy as well as changes in the expression of IFN-regulated genes. Reverse transcriptase inhibitor use in humans attenuated the changes in IFN-regulated genes and was associated with the development of anemia during pregnancy.

CONCLUSION: Our data suggest that retrotransposons have been co-opted in mice and humans to activate HSCs and erythropoiesis during the response to hematopoietic stresses. This may occur through the activation of cGAS-STING signaling and IFN-regulated gene expression in HSCs, increasing HSC cell division and splenic erythropoiesis. This may be necessary to avoid anemia during pregnancy in mice and humans. This provides one explanation for why mammals, unlike some other species, did not eliminate active retrotransposons from their genomes during evolution. Our results together with results from other tissues raise the question of whether retrotransposons are broadly derepressed in stem cells and necessary to promote tissue regeneration after injury. ■
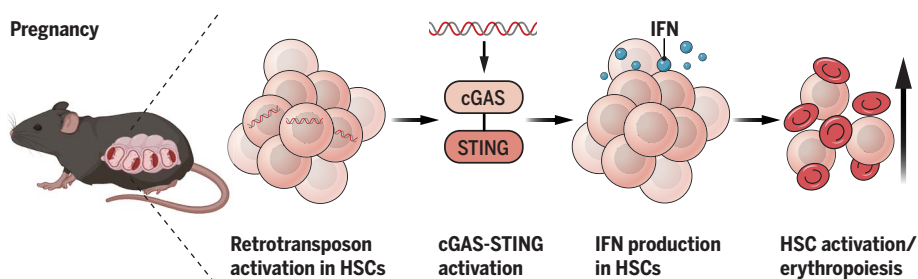
Retrotransposons activate HSCs and increase erythropoiesis in response to hematopoietic stresses. Retrotransposon transcription is activated in HSCs after erythropoietic stresses. This leads to activation of signaling in the cGAS-STING innate immune pathway, which increases IFN production in HSCs. IFN production promotes HSC activation and erythropoiesis. [Image created with BioRender.com.]

READ THE FULL ARTICLE AT
https://doi.org/10.1126/science.ado6836

BLOOD STEM CELLS

Retrotransposons are co-opted to activate hematopoietic stem cells and erythropoiesis

Julia Phan[1], Brandon Chen[1], Zhiyu Zhao[1], Gabriele Allies[2], Antonella Iannaccone[3], Animesh Paul[1], Feyza Cansiz[2], Alberto Spina[3], Anna-Sophia Leven[2], Alexandra Gellhaus[3], Dirk Schadendorf[2], Rainer Kimmig[3], Marcel Mettlen[4], Alpaslan Tasdogan[2]*, Sean J. Morrison[1,5]*

Hematopoietic stem cells (HSCs) and erythropoiesis are activated during pregnancy and after bleeding by the derepression of retrotransposons, including endogenous retroviruses and long interspersed nuclear elements. Retrotransposon transcription activates the innate immune sensors cyclic guanosine 3′,5′-monophosphate–adenosine 5′-monophosphate synthase (cGAS) and stimulator of interferon (IFN) genes (STING), which induce IFN and IFN-regulated genes in HSCs, increasing HSC division and erythropoiesis. Inhibition of reverse transcriptase or deficiency for cGAS or STING had little or no effect on hematopoiesis in nonpregnant mice but depleted HSCs and erythroid progenitors in pregnant mice, reducing red blood cell counts. Retrotransposons and IFN-regulated genes were also induced in mouse HSCs after serial bleeding and, in human HSCs, during pregnancy. Reverse transcriptase inhibitor use was associated with anemia in pregnant but not in nonpregnant people, suggesting conservation of these mechanisms from mice to humans.

Hematopoietic stem cells (HSCs) are activated by hematopoietic stresses to increase blood cell production, though there is a limited understanding of the underlying mechanisms. For example, during pregnancy, estrogen or estrogen receptor signaling activates HSCs, increasing HSC cell division and inducing extramedullary erythropoiesis in the spleen (*1*). This is necessary to maintain red blood cell counts as estrogen receptor deficiency in hematopoietic cells leads to maternal anemia. Serial bleeding also increases erythropoiesis, partly by increasing erythropoietin production (*2, 3*), though erythropoietin is not sufficient to explain the HSC activation or extramedullary hematopoiesis observed after substantial blood loss (*4*).

During embryonic development, sterile inflammation caused by transposable element transcription and interferon (IFN) expression promotes the formation of HSCs (*5–9*). Transposable elements, including DNA transposons and retrotransposons, are germline DNA elements that are capable of moving from one location to another in the genome (*10*). Retro-

transposons, including endogenous retroviruses, long interspersed nuclear elements (LINEs), and short interspersed nuclear elements (SINEs), encode reverse transcriptase, which reverse transcribes retrotransposon transcripts into DNA, enabling reinsertion into the genome. The RNA and/or reverse-transcribed DNA that are produced as a result of transposable element transcription can activate innate immune sensors, including toll-like receptors (*11, 12*), retinoic acid inducible gene I (RIG-I) (*13–15*), melanoma differentiation–associated protein 5 (MDA5) (*16–18*), cyclic guanosine 3′,5′-monophosphate–adenosine 5′-monophosphate synthase (cGAS), and stimulator of IFN genes (STING) (*19–21*). In turn, these innate immune sensors promote the expression of IFN and other proinflammatory cytokines (*22*).

In adult hematopoietic cells, aging (*23, 24*), irradiation (*13, 25*), chemotherapy (*17*), and drugs that inhibit DNA methylation (*18, 26*) or topoisomerase (*27*) lead to DNA damage, changes in chromatin structure, and increased expression of transposable elements. Retrotransposon expression in hematopoietic cells activates inflammatory pathways as a result of signaling by MDA5 (*17*) and RIG-I (*14*), promoting HSC activation after chemotherapy (*17*) or bacterial infection (*28*), though this may undermine long-term HSC function by depleting HSC self-renewal potential (*29–31*). Deficiency for MDA5, cGAS, or STING has little effect on HSC function or hematopoiesis under normal conditions (*17, 28, 32*), raising the question of whether these pathways regulate HSC function or hematopoiesis in normal adult mammals and whether transposons contribute to the regeneration of adult hematopoiesis.

Results

Pregnancy induced retrotransposon transcription in HSCs in mice

To identify transcriptional changes that occur within HSCs during pregnancy, we performed RNA sequencing (RNA-seq) on CD150+ CD48− Lineage− Sca-1+ c-kit+ HSCs and unfractionated cells from the bone marrow and spleens of pregnant dams at embryonic day 14 (E14) of pregnancy as well as from nonpregnant female control mice. We assessed both coding sequences and transposable elements (*33*). In splenic HSCs from pregnant mice compared with bone marrow HSCs from nonpregnant mice, five out of the seven most highly up-regulated gene sets were retrotransposons, including endogenous retroviruses (ERVK, ERVL-MaLR, ERV1, and ERVL families) and LINEs (Fig. 1A). These retrotransposons were transcribed mainly in splenic HSCs, not in bone marrow HSCs, whole bone marrow cells, or whole spleen cells (Fig. 1B and table S1). At earlier stages of pregnancy (E7 to E9), we observed similar results, with increased retrotransposon expression in splenic HSCs from pregnant mice and, to a lesser extent, in bone marrow HSCs and whole bone marrow cells from pregnant mice (Fig. 1C).

We also performed RNA sequencing in splenic HSCs from pregnant mice versus splenic HSCs from nonpregnant mice, along with bone marrow HSCs and unfractionated bone marrow and spleen cells from pregnant and nonpregnant mice (fig. S3A). Gene sets for the LINE, ERVK, and ERVL-MaLR retrotransposon families were enriched in splenic HSCs from pregnant mice as compared to splenic HSCs from nonpregnant mice (fig. S3B), but not in bone marrow HSCs, whole bone marrow, or whole spleen cells from pregnant versus nonpregnant mice. Spleen HSCs from pregnant mice, thus, exhibited increased retrotransposon expression compared with spleen HSCs from nonpregnant mice.

To address whether retrotransposons were derepressed in other hematopoietic progenitors besides HSCs, we performed RNA sequencing on megakaryocyte-erythroid progenitors (MEPs), CD71+ Ter119+ erythroid progenitors, and unfractionated cells from the bone marrow and spleens of pregnant dams (fig. S3C). Retrotransposon expression did not increase during pregnancy in CD71+ Ter119+ cells or unfractionated cells from the bone marrow or spleen (fig. S3, A to C). However, we did observe increased LINE expression in bone marrow MEPs from pregnant compared with nonpregnant mice (fig. S3D). This suggests that retrotransposons were derepressed mainly in HSCs during pregnancy and, to a lesser extent, in some hematopoietic progenitors.

To test whether estrogen contributed to the derepression of retrotransposons during pregnancy, we treated mice with estradiol or vehicle. Consistent with our prior study (*1*), estradiol (2 μg/day for 6 days) administration increased

[1]Children's Research Institute and the Department of Pediatrics, University of Texas Southwestern Medical Center, Dallas, TX 75390, USA. [2]Department of Dermatology, University Hospital Essen & German Cancer Consortium, Essen, & National Center for Tumor Diseases (NCT-West), Campus Essen & Research Alliance Ruhr, Research Center One Health, University Duisburg-Essen, Campus Essen, Essen, Germany. [3]Department of Gynecology and Obstetrics, University Hospital Essen, 45147 Essen, Germany. [4]Department of Cell Biology, University of Texas Southwestern Medical Center, Dallas, TX 75235, USA. [5]Howard Hughes Medical Institute, University of Texas Southwestern Medical Center, Dallas, TX 75390, USA.
*Corresponding author. Email: sean.morrison@utsouthwestern.edu (S.J.M.); alpaslan.tasdogan@uk-essen.de (A.T.)

Fig. 1. Retrotransposon transcription increases in HSCs during pregnancy. (**A** and **B**) We performed RNA-seq in bone marrow HSCs and unfractionated bone marrow and spleen cells from pregnant and non-pregnant female mice as well as spleen HSCs from pregnant mice (spleen HSCs are very rare in nonpregnant mice). (A) Five out of the seven most highly enriched gene sets in spleen HSCs from pregnant dams (E14) compared with bone marrow HSCs from non-pregnant mice were endogenous retrotransposon sequences from multiple families (normalized enrichment score > 2, FDR < 0.01). (B) The list of retrotransposons that differed (log2 fold change > 1, FDR < 0.05) among the cell populations in the analysis showed that retrotransposons were broadly derepressed in splenic HSCs from pregnant mice. (**C**) We performed a similar analysis in pregnant dams at an earlier stage of pregnancy (E7 to E9) and again found a broad derepression (log2 fold change > 1, FDR< 0.05) of multiple families of retrotransposons in splenic HSCs from pregnant dams. Some of these retrotransposons were also more highly expressed in bone marrow HSCs from pregnant compared with that from nonpregnant

mice. (**D**) The percentage of HSCs that incorporated a 72-hour pulse of BrdU in estradiol-treated or vehicle control mice (three mice per treatment). (**E** and **F**) The frequencies (E) and numbers (F) of CD71+ Ter119+ erythroid progenitors in the spleens of estradiol-treated or control mice (a total of seven mice per treatment from three independent experiments). The flow cytometry gates are shown in figs. S1 and S2. In (D) to (F), each dot represents a different mouse, and data represent mean ± standard deviation. *$P < 0.05$; **$P < 0.01$; ***$P < 0.001$. (**G**) Retrotransposons that changed (log2 fold change > 1, FDR < 0.05) in expression in bone marrow or spleen HSCs from estradiol-treated compared with that from untreated control mice.
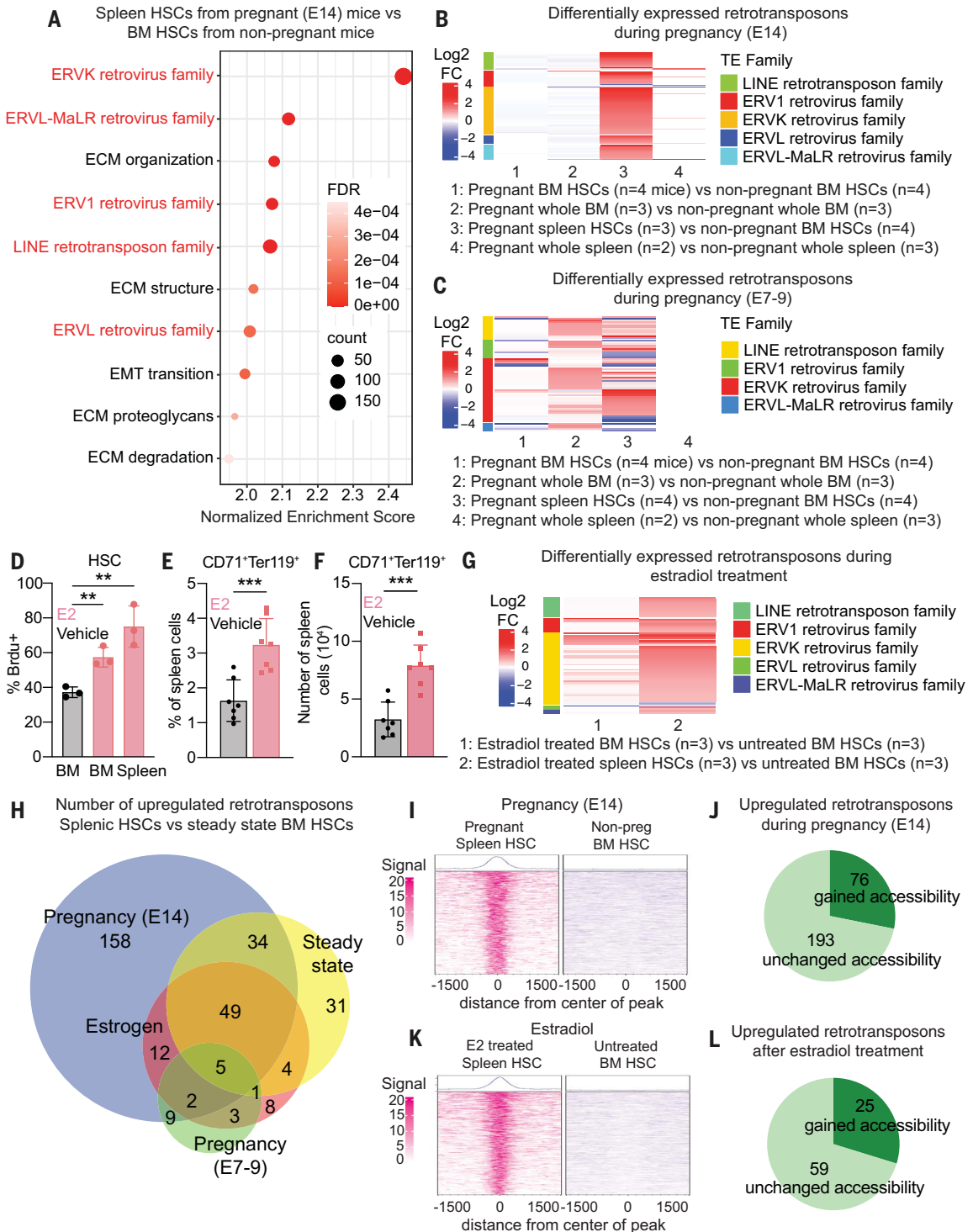
(**H**) Venn diagram showing the overlap of retrotransposons that were increased in expression (log2 fold change > 1, FDR < 0.05) in splenic HSCs from pregnant (E14) mice, normal nonpregnant mice (steady state), early (E7 to E9) pregnant mice, and estradiol-treated mice all compared with bone marrow HSCs from normal, nonpregnant mice. (**I** and **J**) ATAC-seq of spleen HSCs from pregnant mice compared with bone marrow HSCs from nonpregnant mice showing differentially accessible regions (I) and the number of up-regulated retrotransposons in spleen HSCs from pregnant mice that overlap with genomic regions that gained accessibility (J). (**K** and **L**) ATAC-seq of spleen HSCs from estradiol-treated mice compared with bone marrow HSCs from

untreated mice showing differentially accessible regions (K) and the number of up-regulated retrotransposons in spleen HSCs from estradiol-treated mice that overlapped with genomic regions that gained accessibility (L). The numbers of mice from which cells were isolated for RNA-seq is shown in (B), (C), and (G). To isolate spleen HSCs from normal nonpregnant mice, spleens were pooled

from 7 to 12 mice per replicate for a total of three replicates (H). The statistical significance of differences among treatments was assessed by using Student's *t* tests with Holm-Sidak's multiple comparisons adjustments (D) and Student's *t* tests [(E) and (F)]. All statistical tests were two sided. BM, bone marrow; Non-preg, nonpregnant.

cell division by HSCs in the bone marrow and spleen (Fig. 1D) as well as erythropoiesis in the spleen (Fig. 1, E and F). We performed RNA sequencing on HSCs and unfractionated cells from the bone marrow and spleens of estradiol-treated (2 μg/day for 13 days) versus those of untreated control mice. Retrotransposon expression increased in splenic HSCs and, to a lesser extent, in bone marrow HSCs from estradiol-treated compared with untreated mice (Fig. 1G). Most of the retrotransposons that were up-regulated in HSCs during early (E7 to E9) pregnancy, and nearly all of the retrotransposons that were up-regulated in response to estradiol treatment were also up-regulated during late (E14) pregnancy (Fig. 1H). This suggested that estrogen signaling was part of the mechanism by which retrotransposons are derepressed during pregnancy; however, the number of retrotransposons that were expressed after estradiol treatment was much smaller than during pregnancy (Fig. 1H), suggesting that other mechanisms also contribute.

Serial bleeding of mice also derepressed retrotransposons in HSCs

To test whether other erythropoietic stresses also induced retrotransposon expression in HSCs, we performed RNA sequencing on HSCs and unfractionated cells from the bone marrow and spleens of serially bled and nonbled control mice (fig. S4). Gene sets related to erythropoiesis were enriched in splenic HSCs from serially bled mice compared with bone marrow and spleen HSCs from control mice (fig. S4A). Similar to what we observed during pregnancy, 265 retrotransposons were increased in expression in splenic HSCs from serially bled mice compared with bone marrow HSCs from nonbled mice (fig. S4, B and C). Few retrotransposons were increased in expression in bone marrow HSCs from serially bled mice (fig. S4, B and C). Retrotransposons were expressed in spleen HSCs from serially bled mice at levels that were nearly as high as during pregnancy (Fig. 1B and fig. S4, C and D) and were mainly from the same retrotransposon families (fig. S4, D and E). Our data thus indicated that retrotransposons were derepressed in HSCs after erythropoietic stresses.

The accessibility of loci that encode retrotransposons increased in HSCs during pregnancy

To begin to understand how retrotransposon expression increased during pregnancy, we performed assay for transposase-accessible chromatin (ATAC) sequencing (ATAC-seq) on HSCs from the bone marrow and spleen of pregnant

versus nonpregnant mice (Fig. 1I). We observed little or no change in chromatin accessibility in bone marrow HSCs from pregnant compared with that from nonpregnant mice. Conversely, approximately 1100 genomic regions (0.07% of the genome) were more accessible in spleen HSCs from pregnant mice compared with bone marrow HSCs from nonpregnant mice (Fig. 1I). We used bone marrow HSCs from nonpregnant mice as a comparison, as HSCs were so rare in the spleens of nonpregnant mice that we did not obtain interpretable ATAC-seq profiles. These regions with increased accessibility overlapped with 28% of the retrotransposons that were up-regulated in spleen HSCs from pregnant mice (Fig. 1J). The remaining 72% of up-regulated retrotransposons overlapped with regions that showed a trend toward increased accessibility, but the differences were not statistically significant. No regions became less accessible in spleen HSCs from pregnant mice compared with bone marrow HSCs from nonpregnant mice. Loci that encode retrotransposons thus preferentially became more accessible during pregnancy.

We also performed ATAC-seq comparing spleen HSCs from estradiol-treated mice to bone marrow HSCs from untreated control mice (Fig. 1K). Similar to during pregnancy, there was little or no change in chromatin accessibility in bone marrow HSCs from estradiol-treated mice compared with that of control mice. Approximately 2100 genomic regions (0.22% of the genome) became more accessible in spleen HSCs from estradiol-treated mice compared with bone marrow HSCs from control mice (Fig. 1K; no regions became less accessible). These regions overlapped with 30% of the retrotransposons that were up-regulated in spleen HSCs from estradiol-treated mice (Fig. 1L). The remaining 70% of retrotransposons overlapped with regions that showed a trend toward increased accessibility, but the differences were not statistically significant. Estradiol treatment thus appeared to preferentially increase the accessibility of loci that contain retrotransposons. Estrogen receptor α binding is known to remodel chromatin and increase the accessibility of specific genomic regions (*34*), and chromatin structure regulates the transcription of endogenous retroviruses (*35*). Nonetheless, estradiol may influence the expression of retrotransposons through additional mechanisms.

Antiretroviral treatment reduced HSCs and erythropoiesis during pregnancy

Retrotransposon transcription can lead to the accumulation of DNA-RNA hybrids and double

stranded DNAs in the cytoplasm as a result of reverse transcription (*20, 36*). To test whether reverse transcription contributed to HSC activation and erythropoiesis, we treated nonpregnant and pregnant mice with tenofovir and emtricitabine, reverse transcriptase inhibitors that are used clinically to suppress human immunodeficiency virus (HIV) replication (*37*). These inhibitors also have activity against reverse transcriptases in mouse and human retrotransposons (*38*). In nonpregnant female mice, reverse transcriptase inhibitors had little or no effect on blood cell counts (Fig. 2, A to C) or bone marrow (Fig. 2, D to I) or spleen (Fig. 2, J to O) hematopoiesis, including overall cellularity and the frequencies of HSCs, multipotent progenitors (MPPs), Lineage⁻ Sca-1⁺ c-kit⁺ (LSK) progenitors, MEPs, and CD71⁺ Ter119⁺ erythroid progenitors in the bone marrow and spleen. By contrast, treatment of pregnant dams (E9 to E14) with reverse transcriptase inhibitors reduced red blood cell counts without affecting white blood cell or platelet counts (Fig. 2, A to C). Treatment with reverse transcriptase inhibitors also reduced bone marrow cellularity and the frequency of MEPs in the bone marrow (Fig. 2, D to I) as well as the frequencies of HSCs and LSK cells in the spleen (Fig. 2, J to O). The absolute number of CD71⁺ Ter119⁺ erythroid progenitors declined in the spleens of pregnant mice treated with reverse transcriptase inhibitors (Fig. 2P), as did the rates of HSC cell division in the bone marrow and spleen of pregnant mice (Fig. 2Q).

Consistent with the decrease in HSC frequency in the spleen (Fig. 2K) but not in the bone marrow (Fig. 2E), treatment of pregnant mice with reverse transcriptase inhibitors reduced the reconstituting activity of spleen cells (Fig. 2R) but not of bone marrow cells (fig. S5A) upon competitive transplantation into irradiated mice. Treatment of nonpregnant mice with reverse transcriptase inhibitors had no effect on the reconstituting potential of bone marrow (fig. S5B) or spleen (fig. S5C) cells. Reverse transcription was thus necessary to increase HSC cell division and splenic erythropoiesis and to maintain normal red blood cell counts during pregnancy.

STING signaling promoted HSC proliferation and erythropoiesis during pregnancy

To test whether retrotransposons activated cGAS-STING signaling in HSCs, we performed immunofluorescence analysis using anti–phosphorylated STING (phosphoSTING) antibody on HSCs that were flow cytometrically isolated from the bone marrow and spleens

Fig. 2. Reverse transcriptase inhibitors had no effect on hematopoiesis in nonpregnant mice but decreased splenic HSCs and erythropoiesis in pregnant mice, leading to anemia. Pregnant and nonpregnant female mice were treated with reverse transcriptase inhibitors versus vehicle control [(A) to (P) reflect n = 5 to 7 mice per treatment in two independent experiments; each dot represents a different mouse]. (**A** to **C**) Blood cell counts, (**D** to **I**) bone marrow cellularity in one tibia and one femur (D), and the frequencies of HSCs (E), MPPs (F), LSK cells (G), MEPs (H), and CD71+ Ter119+ erythroid progenitors (I) in the bone marrow. (**J** to **O**) Spleen cellularity (J) and the frequencies of HSCs (K), MPPs (L), LSK cells (M), MEPs (N), and CD71+ Ter119+ erythroid progenitors (O) in the spleen. (**P**) Number of CD71+ Ter119+ erythroid progenitors in the spleen. (**Q**) The percentage of HSCs that incorporated a 72- (nonpregnant) or 24-hour (pregnant) pulse of BrdU in reverse transcriptase inhibitor or vehicle-treated mice (three mice per treatment). (**R**) Donor cell reconstitution of CD45+ hematopoietic cells, Mac-1+ Gr-1+ myeloid cells, B220+ B cells, and CD3+ T cells in the blood of mice that were competitively transplanted with 1.5 × 10^6 donor spleen cells from pregnant dams that were treated with reverse transcriptase inhibitors or vehicle control (three donor mice and a

total of 13 to 14 recipients per treatment in three independent experiments). The flow cytometry gates are shown in figs. S1 and S2. All data represent mean ± standard deviation. *P < 0.05; **P < 0.01; ***P < 0.001. Statistical significance was assessed by using two-way ANOVAs followed by Sidak's multiple comparisons adjustments [(A), (C), and (E) to (O)], Mann-Whitney tests followed by Holm-Sidak's multiple comparisons adjustment (B), Welch's t tests followed by Holm-Sidak's multiple comparisons adjustments [(D) and (P)], a Student's t test [(Q) nonpregnant] and a matched-samples two-way ANOVA followed by Sidak's multiple comparisons adjustment [(Q) pregnant, or nparLD tests followed by Holm-Sidak's multiple comparisons adjustments for overall differences taking into account all time points and Mann-Whitney tests for data at individual time points (R)]. All statistical tests were two-sided. WBC, white blood cell; RBC, red blood cell.
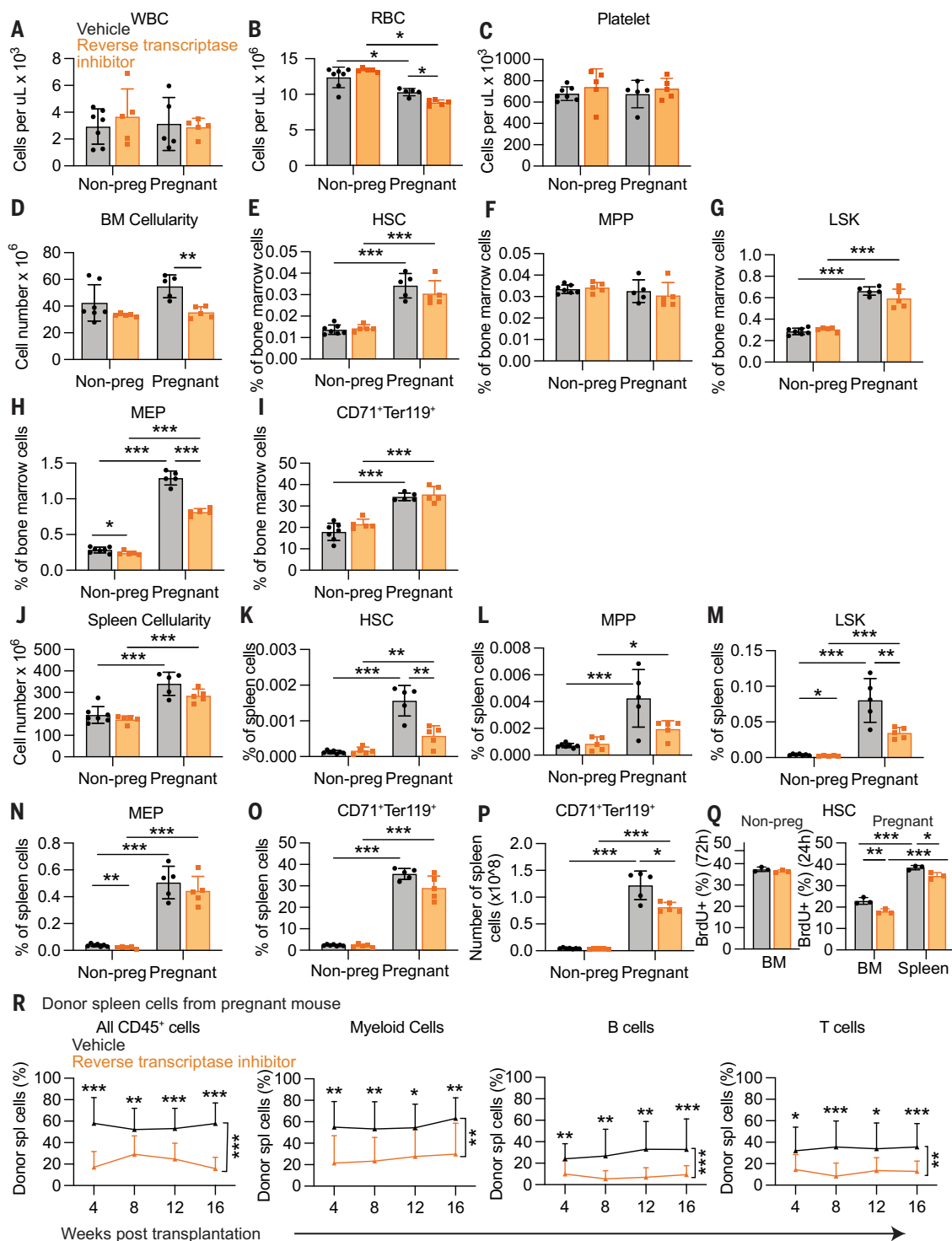
of pregnant and nonpregnant female mice. STING is phosphorylated when activated (*39*). We observed punctate phosphoSTING stain-

ing in the cytoplasm of HSCs from the bone marrow and spleens of pregnant mice at levels that were higher than in HSCs from non-

pregnant mice or *STING*^gt/gt^ mice (fig. S6, A and B). *STING*^gt/gt^ mice have a missense mutation in exon 6, which eliminates the STING protein

(40). Treatment of pregnant mice with reverse transcriptase inhibitors reduced phosphoSTING staining in HSCs from the spleen but not from the bone marrow (fig. S6, C and D). STING was thus activated in HSCs from the bone marrow and spleens of pregnant mice, and reverse transcriptase inhibitors reduced STING activation in the spleen.

To test whether STING was necessary for increased erythropoiesis during pregnancy, we examined $STING^{gt/gt}$ and littermate control mice. In nonpregnant female mice, STING deficiency had no effect on blood cell counts (Fig. 3, A to C), bone marrow (Fig. 3D), or spleen (Fig. 3J) cellularity or the frequencies of HSCs, MPPs, LSK cells, MEPs, or CD71$^+$ Ter119$^+$ erythroid progenitors in the bone marrow (Fig. 3, E to I) or spleen (Fig. 3, K to O). In nonpregnant mice, STING deficiency also had no effect on the rate of HSC cell division (Fig. 3P) or on the reconstituting potential of bone marrow (fig. S7A) or spleen (fig. S7B) cells upon competitive transplantation into irradiated mice. In pregnant mice, STING deficiency reduced red blood cell counts but not white blood cell or platelet counts (fig. 3, A to C). In pregnant mice, STING deficiency did not reduce bone marrow (Fig. 3D) or spleen (Fig. 3J) cellularity, and it had a small, but statistically significant, effect on the frequencies of HSCs and restricted hematopoietic progenitors in the bone marrow (Fig. 3, E to I). STING deficiency reduced the frequencies of HSCs, LSK cells, MEPs, and CD71$^+$ Ter119$^+$ erythroid progenitors in the spleens of pregnant mice to a greater extent (Fig. 3, K to O). STING deficiency also reduced the rates of HSC cell division in the bone marrow and spleens of pregnant mice (Fig. 3P). The reconstituting potential of STING-deficient bone marrow (Fig. 3Q) and spleen (Fig. 3R) cells from pregnant mice was reduced compared with that of control cells from pregnant mice upon competitive transplantation into irradiated mice. STING activation thus contributed to the increased HSC proliferation and erythropoiesis in the spleen during pregnancy such that STING deficiency led to lower red blood cell counts in pregnant mice.

cGAS signaling promoted HSC proliferation and erythropoiesis during pregnancy

In nonpregnant female mice, cGAS deficiency had little or no effect on blood cell counts (Fig. 4, A to C), bone marrow (Fig. 4D) or spleen (Fig. 4J) cellularity, or the frequencies of HSCs, MPPs, LSK cells, MEPs, or CD71$^+$ Ter119$^+$ erythroid progenitors in the bone marrow (Fig. 4, E to I) or spleen (Fig. 4, K to O). cGAS deficiency also had no effect on the rate of HSC cell division (Fig. 3P) or the reconstituting potential of bone marrow (fig. S8B) or spleen (fig. S8C) cells upon competitive transplantation into irradiated mice. Conversely, in pregnant mice, cGAS deficiency reduced red blood cell count but not

white blood cell or platelet counts (Fig. 4, A to C). In pregnant mice, cGAS deficiency did not reduce bone marrow (Fig. 4D) or spleen (Fig. 4J) cellularity but reduced the frequencies of MEPs in the bone marrow (Fig. 4, E to I) as well as HSCs and CD71$^+$ Ter119$^+$ erythroid progenitors in the spleen (Fig. 4, K to O). cGAS deficiency also reduced the rate of HSC cell division in the spleens of pregnant mice (Fig. 4P). The reconstituting potential of cGAS-deficient spleen (Fig. 4Q) but not bone marrow (fig. S8A) cells from pregnant mice was reduced compared with that of control cells from pregnant mice. cGAS activation thus contributed to increased HSC cell division and erythropoiesis in the spleen during pregnancy.

cGAS-STING signaling promoted IFN expression in HSCs from pregnant mice

cGAS-STING activation leads to the production of IFNs (19, 41, 42). An acute increase in IFN-α production promotes HSC proliferation, whereas chronic IFN-α production erodes HSC self-renewal potential and depletes HSCs (30, 43). To test whether IFNs increased during pregnancy, we performed enzyme-linked immunosorbent assays (ELISAs) for IFN-α in blood plasma, bone marrow lysate, and spleen lysate from female wild-type, $STING^{gt/gt}$, and $Vav1$-$iCre;cGAS^{fl/fl}$ mice that were pregnant or nonpregnant. Pregnancy increased IFN-α levels in bone marrow and spleen lysate but not blood plasma from wild-type mice (fig. S9, A to F). These increases were not detected in $STING^{gt/gt}$ or $Vav1$-$iCre;cGAS^{fl/fl}$ mice (fig. S9, A to F). We did not detect increases in the levels of other inflammatory cytokines in blood plasma, bone marrow, or spleen lysate from pregnant compared with nonpregnant mice (fig. S10). Therefore, there was a cGAS-STING–dependent increase in IFN-α levels during pregnancy, particularly in the spleen.

Given the increase in IFN levels during pregnancy, we assessed the expression of IFN-regulated genes by RNA-seq. We observed changes in the expression of IFN-regulated genes in splenic HSCs from pregnant mice compared with splenic HSCs and bone marrow HSCs from nonpregnant mice (columns 6 and 8, Fig. 5A). Some IFN-regulated genes increased in expression (red, Fig. 5A), and some decreased in expression (blue, Fig. 5A), as expected for IFN-regulated genes (44, 45). $STING$ deficiency largely eliminated these changes in HSCs from pregnant mice (columns 7 and 9, Fig. 5A). We observed little change in the expression of IFN-regulated genes in bone marrow HSCs from pregnant mice compared with that from nonpregnant mice (columns 1 and 2, Fig. 5A). We observed more limited changes in the expression of IFN-regulated genes in whole bone marrow and whole spleen cells from pregnant mice compared with that from nonpregnant mice (columns 4 and 11, Fig. 5A).

We observed larger changes in the expression of IFN-regulated genes in whole bone marrow and whole spleen cells from pregnant $STING$-deficient mice compared with that from nonpregnant mice (columns 5 and 12, Fig. 5A). $STING$-deficient mice have defects in the expression of anti-inflammatory factors that exacerbate inflammation in some circumstances (46). The data suggest that STING is necessary in HSCs for most of the changes in IFN-regulated gene expression that are induced by pregnancy but that STING negatively regulates IFN responses in some other cells in the bone marrow and spleen.

Although we did not observe an increase in IFN-γ levels in plasma, bone marrow, or spleen lysate during pregnancy, multiple gene sets related to type II IFN signaling were enriched in spleen HSCs from pregnant mice compared with spleen HSCs from nonpregnant mice (fig. S10D). IFN-γ signaling thus increased in HSCs but did not increase systemically during pregnancy.

Spleen HSCs from estradiol-treated mice and serially bled mice also showed changes in the expression of IFN-regulated genes compared with bone marrow and spleen HSCs from untreated control mice (fig. S9, G and H).

With RNA-seq, we did not detect the expression of IFN transcripts in HSCs or unfractionated cells from the bone marrow or spleen of pregnant or nonpregnant mice. Given that IFNs can be difficult to detect by RNA-seq, we also assessed this by reverse transcription quantitative polymerase chain reaction (RT-qPCR). With RT-qPCR, we found that $Ifna$ (which encodes IFN-α) was elevated in HSCs from the bone marrow and spleen of pregnant mice compared with HSCs in the bone marrow and spleen of nonpregnant mice (fig. S11, A and B). However, we did not detect increased $Ifna$ expression in unfractionated cells, LK myeloid progenitors, CD3$^+$ T cells, B220$^+$ B cells, or Mac-1$^+$ Gr-1$^+$ myeloid cells in the bone marrow or spleen of pregnant mice (fig. S11, A and B). The increase in $Ifna$ expression in spleen HSCs during pregnancy was not observed in $STING^{gt/gt}$ mice (fig. S11, C and D). These data suggest that cGAS-STING signaling promoted $Ifna$ expression in HSCs during pregnancy.

Type I IFN contributed to the increase in splenic erythropoiesis

To test whether the effects of cGAS-STING signaling on HSCs and erythropoiesis during pregnancy were partly mediated by type-I IFN I (IFN-α or IFN-β), we examined $Ifnar1^{-/-}$ mice, which lack type-I IFN receptor function (47). In nonpregnant female mice, $Ifnar1$ deficiency did not affect blood cell counts (fig. S11, E to G), bone marrow (fig. S11H) or spleen (Fig. 5B) cellularity, or the frequencies of HSCs, MPPs, MEPs, or CD71$^+$ Ter119$^+$ erythroid progenitors in the bone marrow (fig. S11, I to M)
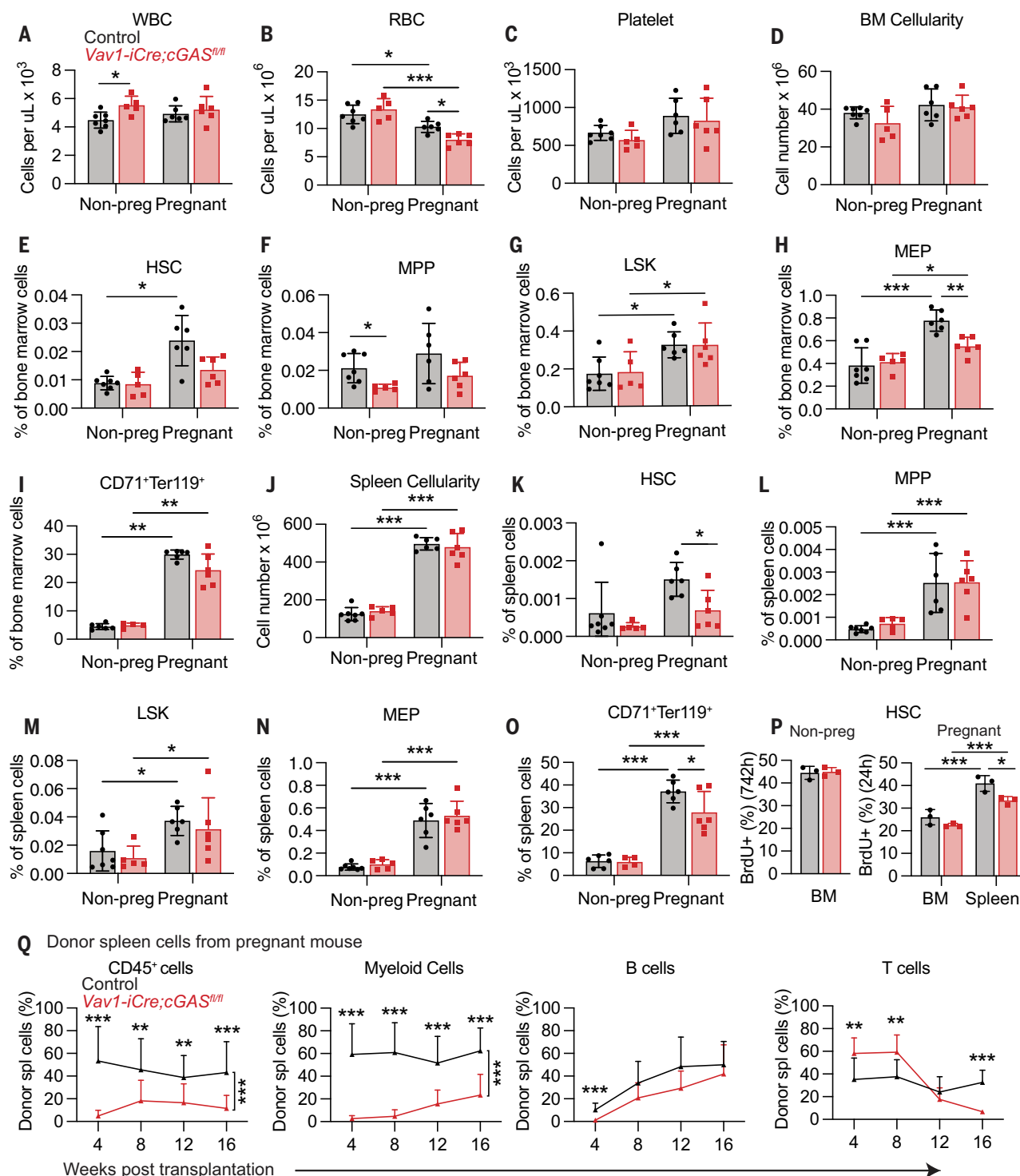
Fig. 3. STING is necessary to increase HSC frequency and erythropoiesis during pregnancy. We assessed hematopoiesis in pregnant or nonpregnant female *STING*^gt/gt^ or littermate control mice (all panels reflect 4 to 13 mice per treatment in four independent experiments; each dot represents a different mouse). (**A** to **C**) Blood cell counts, (**D** to **I**) bone marrow cellularity in one tibia and one femur (D), and the frequencies of HSCs (E), MPPs (F), LSK cells (G), MEPs (H), and CD71⁺ Ter119⁺ erythroid progenitors (I) in the bone marrow. (**J** to **O**) Spleen cellularity (J) and the frequencies of HSCs (K), MPPs (L), LSK cells (M), MEPs (N), and CD71⁺ Ter119⁺ erythroid progenitors (O) in the spleen. (**P**) The percentage of HSCs that incorporated a 72- (nonpregnant) or 24-hour (pregnant) pulse of BrdU in *STING*^gt/gt^ and littermate control mice (four mice per treatment in two independent experiments). (**Q**) Donor cell reconstitution of CD45⁺ hematopoietic cells, Mac-1⁺ Gr-1⁺ myeloid cells, B220⁺ B cells, and CD3⁺ T cells in the blood of mice that were competitively transplanted with 5 × 10⁵ donor bone marrow cells from pregnant *STING*^gt/gt^ or littermate control dams (three donor mice were transplanted into a total of 13 to 14 recipi-

ents per genotype in three independent experiments). (**R**) Donor cell reconstitution in the blood of mice that were competitively transplanted with 1.5 × 10⁶ donor spleen cells from pregnant *STING*^gt/gt^ or littermate control dams (three donor mice were transplanted into a total of 11 to 12 recipients per genotype in three independent experiments). The flow cytometry gates are shown in figs. S1 and S2. All data represent mean ± standard deviation. *P < 0.05; **P < 0.01; ***P < 0.001. Statistical significance was assessed by using two-way ANOVAs followed by Sidak's multiple comparisons adjustments [(A) to (B), (D) to (K), and (M)],
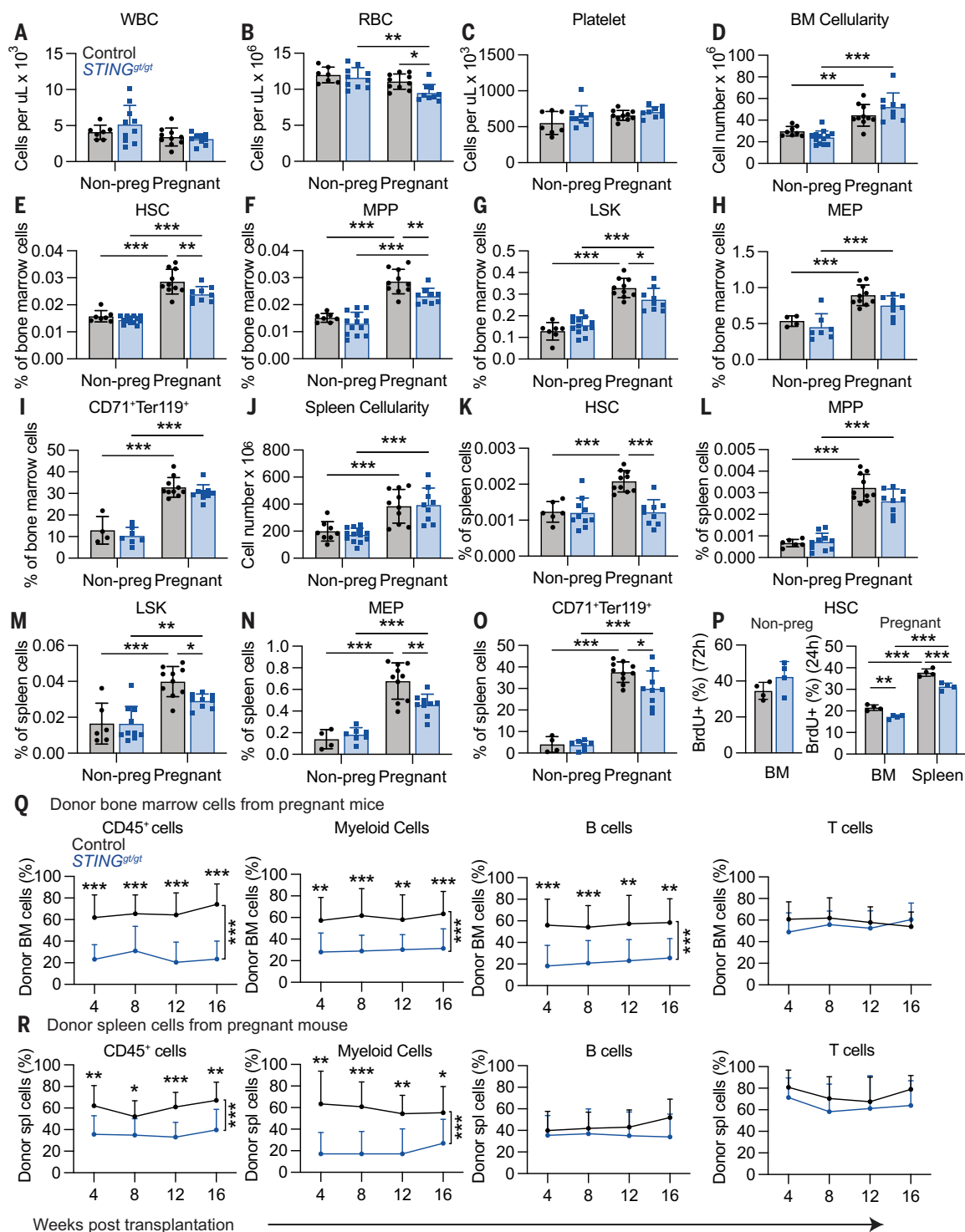
Welch's *t* tests followed by Holm-Sidak's multiple comparisons adjustments [(C), (L), and (O)], multiple Student's *t* tests followed by Holm-Sidak's multiple comparisons adjustments (N), a Student's *t* test [(P) nonpregnant] and a matched-samples two-way ANOVA followed by Sidak's multiple comparisons adjustment [(P) pregnant], or nparLD tests followed by Holm-Sidak's multiple comparisons adjustments for overall differences taking into account all time points and Mann-Whitney tests for data at individual time points [(Q) and (R)]. All statistical tests were two-sided.

Fig. 4. cGAS is necessary to increase HSC frequency and erythropoiesis during pregnancy. We assessed hematopoiesis in pregnant or nonpregnant female *Vav1-iCre;cGAS*fl/fl or littermate control mice (all panels reflect four to seven mice per treatment in three independent experiments; each dot represents a different mouse). (**A** to **C**) Blood cell counts, (**D** to **I**) bone marrow cellularity in one tibia and one femur (D), and the frequencies of HSCs (E), MPPs (F), LSK cells (G), MEPs (H), and CD71+ Ter119+ erythroid progenitors (I) in the bone marrow. (**J** to **O**) Spleen cellularity (J) and the frequencies of HSCs (K), MPPs (L), LSK cells (M), MEPs (N), and CD71+ Ter119+ erythroid progenitors (O) in the spleen. (**P**) The percentage of HSCs that incorporated a 72- (nonpregnant) or 24-hour

(pregnant) pulse of BrdU in *Vav1-iCre;cGAS*fl/fl or littermate control mice (three mice per treatment). (**Q**) Donor cell reconstitution of CD45+ hematopoietic cells, Mac-1+ Gr-1+ myeloid cells, B220+ B cells, and CD3+ T cells in the blood of mice that were competitively transplanted with 1.5 × 10^6 donor spleen cells from pregnant *Vav1-iCre;cGAS*fl/fl or littermate control dams (three donor mice were transplanted into a total of 12 to 13 recipients per genotype in three independent experiments). The flow cytometry gates are shown in figs. S1 and S2. All data represent mean ± standard deviation. *P < 0.05; **P < 0.01; ***P < 0.001. Statistical significance was assessed by using two-way ANOVAs followed by Sidak's multiple comparisons adjustments [(A) to (D), (J), and

(L) to (O)], Mann-Whitney tests followed by Holm-Sidak's multiple comparisons adjustments [(E), (I), and (K)], multiple Student's *t* tests followed by Holm-Sidak's multiple comparisons adjustments [(F) to (H) and (K)], a Student's *t* test [(P) nonpregnant] and a matched-samples two-way ANOVA followed by Sidak's multiple comparisons adjustment [(P) pregnant], or nparLD tests followed by Holm-Sidak's multiple comparisons adjustments for overall differences taking into account all time points and Mann-Whitney tests for data at individual time points (Q). All statistical tests were two-sided.
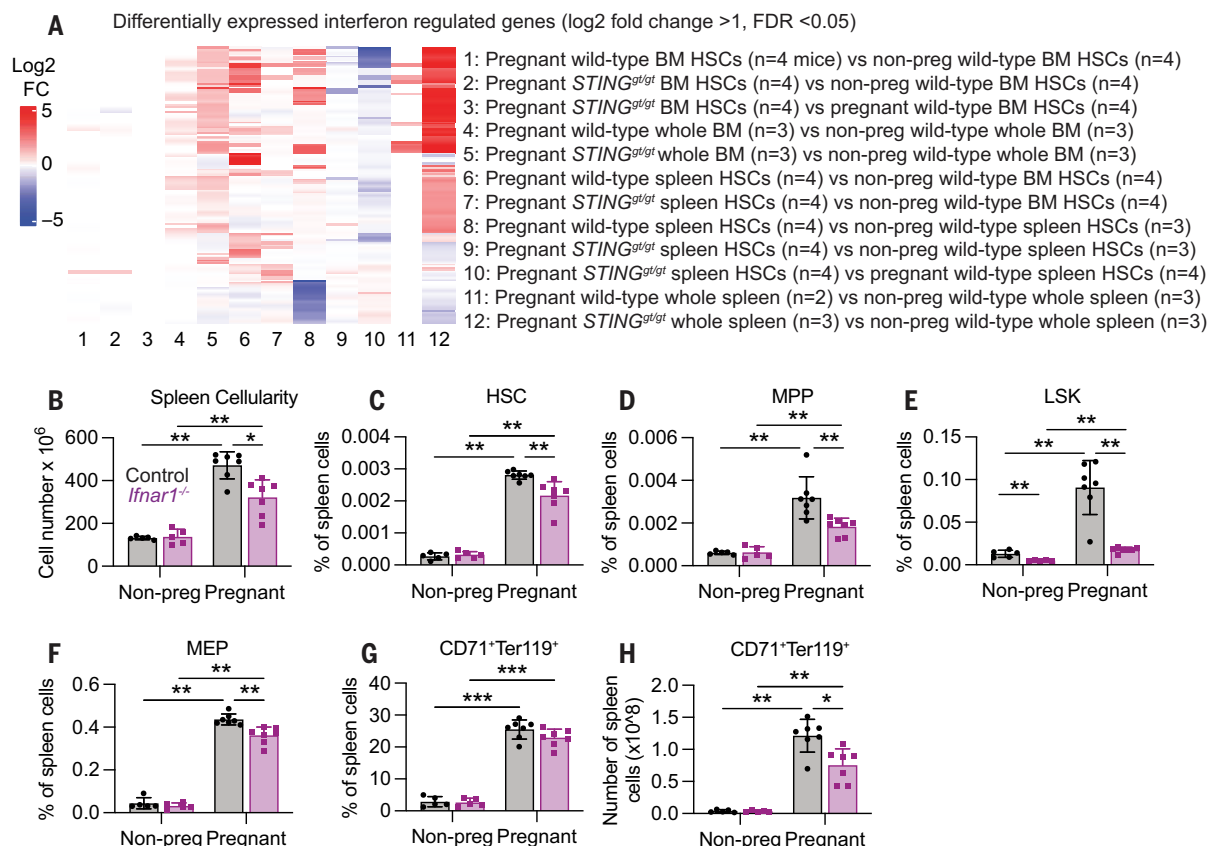
Fig. 5. STING-dependent IFN expression increases during pregnancy and promotes splenic erythropoiesis. (**A**) Changes in IFN-regulated gene expression among bone marrow and spleen HSCs as well as unfractionated bone marrow and spleen cells from pregnant and nonpregnant female *STING*^gt/gt and littermate wild-type mice. (**B** to **H**) Spleen cellularity (B) and the frequencies of HSCs (C), MPPs (D), LSK cells (E), MEPs (F), and CD71$^+$ Ter119$^+$ erythroid progenitors (G) as well as the number of CD71$^+$ Ter119$^+$ erythroid progenitors (H) in the spleen of pregnant or nonpregnant female *Ifnar1*$^{-/-}$ or littermate control mice. Each dot represents a different mouse (five to seven mice per treatment in four independent experiments). The flow cytometry gates are shown in fig. S2. All data represent mean ± standard deviation. *$P < 0.05$; **$P < 0.01$; ***$P < 0.001$. Statistical significance was assessed by using Mann-Whitney tests followed by Holm-Sidak's multiple comparisons adjustments [(B) to (F) and (H)] or two-way ANOVAs followed by Sidak's multiple comparisons adjustments (G).

or spleen (Fig. 5, C to H). In pregnant mice, *Ifnar1* deficiency reduced spleen cellularity (Fig. 5B) and the frequencies of HSCs, MPPs, LSK cells, and MEPs in the spleen (Fig. 5, C to F). *Ifnar1* deficiency did not reduce the frequency of CD71$^+$ Ter119$^+$ erythroid progenitors in the spleen (Fig. 5G), but it did reduce the absolute number of CD71$^+$ Ter119$^+$ erythroid progenitors (Fig. 5H), consistent with the reduction in spleen cellularity (Fig. 5B). Type I IFN thus contributed to the increase in splenic erythropoiesis during pregnancy. We did not observe a decline in red blood cell counts in *Ifnar1*-deficient mice (fig. S11F), indicating that other mechanisms also contributed to the effects of cGAS-STING signaling on erythropoiesis during pregnancy, potentially including type-II IFN, which can be induced by type-I IFN (*48*).

Retrotransposons were derepressed in HSCs during pregnancy in humans

To test whether retrotransposons are derepressed in humans during pregnancy, we performed RNA-seq on Lineage⁻CD34$^+$ CD38$^-$ cells, which are highly enriched for HSCs (*49*), from the blood of pregnant and nonpregnant females. The two most highly enriched gene sets in HSCs from pregnant compared with nonpregnant females were LINE and SINE retrotransposons (Fig. 6A), the most active retrotransposon families in humans (*50*). The third and fourth most highly enriched gene sets related to a vaccine immune response, including several IFN-regulated genes (*51*) and erythropoiesis (*52*) (Fig. 6A). During pregnancy, the increase in retrotransposon transcription in HSCs did not occur uniformly, as approxi-

mately one-third of HSC samples (each from a different person) did not exhibit clear increases in retrotransposon transcription (Fig. 6B). HSCs with higher LINE and SINE expression had more pronounced changes in the expression of IFN-regulated genes than those with low LINE and SINE transcription (Fig. 6C). Human HSCs thus also exhibited increased retrotransposon transcription and changes in the expression of IFN-regulated genes during pregnancy.

We also performed RNA-seq on Lineage⁻ CD34$^+$ CD38$^-$ cells from the blood of three pregnant people with HIV who were undergoing treatment with reverse transcriptase inhibitors. HIV viral load was undetectable in these individuals, indicating that it was well controlled (*53*). HSCs from two of these people

Fig. 6. Retrotransposon expression is increased in HSCs during pregnancy in humans and was associated with the development of anemia. (**A**) Gene set enrichment analysis on RNA sequencing data from Lin$^-$ CD34$^+$ CD38$^-$ cells isolated from the blood of pregnant and nonpregnant females. (**B**) Changes in retrotransposon expression in Lin$^-$ CD34$^+$ CD38$^-$ cells from the blood of pregnant females (n = 11, 3 of which were taking reverse transcriptase inhibitors; GA, gestational age) compared with average values from Lin$^-$ CD34$^+$ CD38$^-$ cells obtained from nonpregnant females (n = 3). (**C**) Differential expression of IFN-regulated genes in Lin$^-$ CD34$^+$ CD38$^-$ cells from pregnant compared with that from nonpregnant females. HSCs were categorized based on high LINE or SINE expression and no reverse transcriptase inhibitor treatment (column 1),

low LINE or SINE expression and no reverse transcriptase inhibitor treatment (column 2), all reverse transcriptase inhibitor treated without regard to LINE or SINE expression (column 3), and reverse transcriptase inhibitor treated and high LINE or SINE expression (column 4). (**D** to **F**) Blood cell counts from individuals with and without reverse transcriptase inhibitor treatment, before and during pregnancy; lines connect the same individual. The flow cytometry gates are shown in fig. S12. All data represent mean ± standard deviation. *P < 0.05; **P < 0.01; ***P < 0.001. Statistical significance was assessed by using paired t tests followed by Holm-Sidak's multiple comparisons adjustments [(D) to (F)]. All statistical tests were two sided. RTi, reverse transcriptase inhibitor.
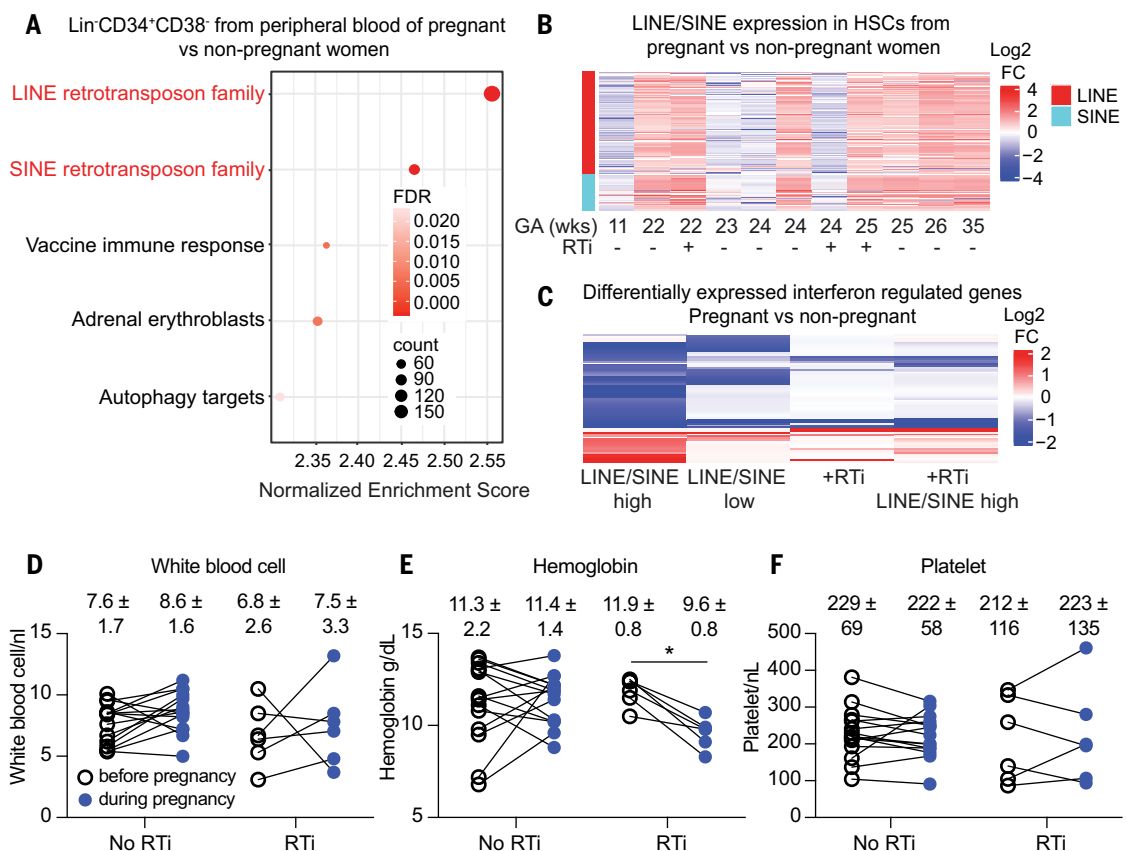
exhibited increased transcription of retrotransposons relative to HSCs from nonpregnant females (Fig. 6B). However, the HSCs from pregnant females taking reverse transcriptase inhibitors exhibited many fewer changes in the expression of IFN-regulated genes compared with HSCs from females not taking reverse transcriptase inhibitors, even when only HSCs with strong LINE and SINE expression were considered (Fig. 6C).

We retrospectively assessed blood cell counts before and during pregnancy in 15 individuals who did not take reverse transcriptase inhibitors and in 6 who did. Those who were not taking reverse transcriptase inhibitors did not exhibit statistically significant changes in white blood cell or platelet counts or hemoglobin levels during pregnancy compared to that of before pregnancy (Fig. 6, D to F). Individuals taking reverse transcriptase inhibitors did not exhibit changes in white blood cell or platelet counts during pregnancy (Fig. 6, D and F); however, they did exhibit declines in hemoglobin levels during pregnancy, such that they all became anemic (Fig. 6E). These

data suggested that humans also derepress retrotransposons during pregnancy to activate innate immune pathways in HSCs and to promote erythropoiesis.

Discussion

Our findings show that retrotransposons are derepressed in HSCs during pregnancy, activating cGAS-STING signaling and triggering an IFN response that promotes HSC activation and increases erythropoiesis. Our data suggested that this is necessary to avoid anemia during pregnancy in mice and humans. The observation that retrotransposons were also derepressed in HSCs from serially bled mice suggests that these mechanisms are broadly used to increase HSC function and erythropoiesis in response to erythropoietic stresses. This is surprising given that retrotransposon expression declines in mature blood cells during pregnancy (*54*) and given the potential for retrotransposon-mediated mutagenesis (*55*); however, additional studies will be required to test whether the derepression of retrotransposons in HSCs actually increases retrotransposon-

mediated mutagenesis or whether such mutations are propagated to differentiated hematopoietic cells.

Treatment with estradiol increased retrotransposon transcription and chromatin accessibility at loci that overlap with retrotransposons. However, many more retrotransposons increased in expression during pregnancy compared with after estradiol treatment. Moreover, retrotransposons were also derepressed after serial bleeding, which would not be expected to be mediated by changes in estrogen. Therefore, there are likely to be additional, estrogen-independent mechanisms that promote retrotransposon expression after erythropoietic stresses.

cGAS–STING–IFN-α signaling does not appear to be entirely responsible for the effects of retrotransposons on erythropoiesis during pregnancy. cGAS-STING signaling may induce additional IFNs beyond IFN-α. cGAS-STING signaling may also have IFN-independent effects on HSCs and erythropoiesis, as cGAS-STING can also regulate cell death (*56*), proliferation (*57*), and autophagy (*58*) through

IFN-independent mechanisms. It is possible that other innate immune pathways contribute to the effect of retrotransposons on HSCs and erythropoiesis.

In humans, females taking reverse transcriptase inhibitors exhibited lower hemoglobin levels during pregnancy, in contrast to those who did not take reverse transcriptase inhibitors. This is consistent with a report that people with HIV who take reverse transcriptase inhibitors are much more likely to become anemic during pregnancy than those who do not (59). HIV disease may contribute to anemia, but the individuals in our study were asymptomatic with well-controlled disease and undetectable viral loads. Nonpregnant, asymptomatic, HIV-infected females have a similar incidence of anemia as the general population (60). Our data raise the possibility that reverse transcriptase inhibitor use promotes the development of anemia in pregnant humans by inhibiting the activation of innate immune pathways by retrotransposons; however, additional studies will be required in larger numbers of patients from more institutions to evaluate this.

Commensal microbiota induce endogenous retroviruses in keratinocytes, activating cGAS-STING signaling and recruiting T cells that promote immunity and wound repair (21). Considering this observation, our results raise the question of whether retrotransposons are commonly derepressed in stem cells after tissue injury and whether this contributes widely to tissue regeneration.

Materials and Methods
Reagents

The markers used for the identification of the cell populations examined in this study can be found in table S2 and details related to antibodies and primer sequences can be found in tables S3 and S4, respectively.

Mice

All mouse experiments complied with all relevant ethical regulations and were performed according to protocols approved by the Institutional Animal Care and Use Committee at the University of Texas Southwestern Medical Center (protocol 2019-102632-G). *Vav1-iCre* (JAX stock #008610) (61) and *Ifnar1*$^{-/-}$ (JAX stock #028288) (62) mice were obtained from Jackson Laboratory. *STING*$^{gt/gt}$ mice (JAX stock #017537) (40) and *cGAS*$^{fl/fl}$ mice were obtained from Zhijian Chen (UT Southwestern). All mice were analyzed between 7 and 16 weeks of age unless otherwise indicated. All mice were backcrossed at least four times onto a C57BL/Ka (CD45.2) background. All mice were analyzed between 7 and 16 weeks of age unless otherwise indicated. Most experiments involved only female mice, such as experiments involving pregnancy and bleed-

ing. Experiments with reverse transcriptase inhibitors and *STING* and *cGAS* deficiency in nonpregnant conditions involved male and female mice. For transplantation assays, C57BL/Ka-Thy-1.1/C57BL/Ka-Thy-1.2 (CD45.2/CD45.2) mice were used as recipients and C57BL/Ka-Thy-1.2 (CD45.1) mice were used as a source of competitor bone marrow cells. Mice were housed at the Animal Resource Center at the University of Texas Southwestern Medical Center in AAALAC-accredited, specific-pathogen-free animal care facilities under a 12 hour:12 hour light:dark cycle with a temperature of 18° to 24°C and humidity of 35 to 60%. Mice were housed with a maximum of 5 same-sex mice per cage. Breeding cages had one male and two females. Igloos and bedding were placed in each cage for enrichment. Mice were fed normal chow (Teklad Global 16% Protein Rodent Diet; Envigo #2016). Mice were euthanized using isoflurane, and cervical dislocation was used as a secondary method of euthanasia.

RNA-seq in mouse hematopoietic cells

Cells were sorted into RLT buffer plus (Qiagen RNeasy Plus Micro kit) and RNA was purified according to the manufacturer's instructions. RNA quality was validated using a Pico Bioanalyzer. Libraries were generated using SMARTer Stranded Total RNA-Seq kit – v2 Pico Input Mammalian (Takara). Library fragment size was measured using D1000 Screen Tape (Agilent) and libraries were quantified using the Qubit dsDNA high-sensitivity assay kit (Life Technologies). Libraries were sequenced using an Illumina NextSeq 500 with 200 base pair paired-end sequencing. The quality of RNA-seq raw reads was checked using FastQC 0.11.8. Raw reads were trimmed using TrimGalore 0.6.4 and mapped to the Ensembl GRCm38 mouse reference genome using STAR2.7.9a. Mapped reads were quantified using TETranscripts 2.2.1. Quantified mapped reads were normalized using DESeq2 1.30.0 with R 4.0.2. Differential expression was assessed using DESeq 2 1.30.0. Gene set enrichment analyses were performed using GSEA 4.1.0. Dot plots showing gene set enrichment analyses were made in R using the ggplot2 package. Venn diagrams showing the overlap in retrotransposons that were up-regulated under various conditions were made using DeepVenn (63). Heatmaps showing the fold-change of retrotransposons or IFN regulated genes that were differentially expressed among conditions or cells were made in R using the ggplots2 and pheatmap packages. The heatmaps in Fig. 5A and fig. S8, G and H show all mouse IFN-regulated genes [based on interferome.com (64)] that were differentially expressed (log2 fold change >1, FDR < 0.05) among cells. The heatmap in Fig. 5K shows all human IFN response genes (64) that were differentially expressed among samples.

Retrotransposon gene sets were from TETranscripts 2.2.1 while all other gene sets were from the Molecular Signature Database (MSigDB). In Fig. 1A, the ECM organization gene set was annotated as "Reactome extracellular matrix organization" in MSigDB, the ECM structure gene set was annotated as "GOMF extracellular matrix structural constituent" in MSigDB, the EMT transition gene set was annotated as "Hallmark epithelial mesenchymal transition" in MSigDB, the ECM proteoglycan gene set was annotated as "Reactome ecm proteoglycans" in MSigDB, and the ECM degradation gene set was annotated as "Reactome degradation of the extracellular matrix" in MSigDB.

ATAC-seq

Three replicates of 1000 CD150$^+$CD48$^-$Lineage$^-$Sca-1$^+$c-kit$^+$ cells per replicate were isolated by flow cytometry from different mice and sorted into MACS freezing solution (Milentenyi Biotec). Libraries for ATAC sequencing were prepared as described (65). The libraries were sequenced using 200–base pair (bp) paired-end reads with an Illumina NextSeq 500. Adapter sequences were trimmed using Cutadapt 2.5. Bowtie2 2.1.0 was used to align reads to the Ensembl GRCm38 mouse reference genome. Samtools 1.18 was used for data filtering and file format conversion. Blacklist regions and mitochondrial DNA were removed before peak calling. The genomic location of peaks was determined using Genrich 0.6.1. Differentially accessible peaks were identified using DiffBind 3.2.5 with default parameters. Peaks that were enriched (fold change > 2, FDR < 0.05) were considered to gain accessibility. Peaks were considered to overlap with genes or retrotransposons if at least part of the peak fell between 1000 bp upstream of the transcription start site and the end of the gene or retrotransposon.

Serial bleeding

Two- to three-month-old female mice were bled via the tail vein five times over a 12 day period, removing approximately 200 μl of blood each time. Mice were analyzed 2 days after the last bleed.

Drug treatments

Mice were treated with estradiol by injecting subcutaneously with 2 μg/day of E2 (Sigma-Aldrich) in corn oil (Sigma-Aldrich). Mice were analyzed 1 day after the last injection. In Fig. 1, D to F, male mice were injected with E2 for 6 days and male controls were injected with corn oil. In Fig. 1, G and H, female mice were injected for 13 days. To treat with reverse transcriptase inhibitors, we made a stock solution in PBS that contained 12.5 mg/ml of tenofovir disoproxil fumarate and 7.5 mg/ml of emtricitabine (both from ACROS organics). We then administered to mice by gavaging with this

solution daily for 5 days such that the mice received 100 mg/kg body mass/day of tenofovir and 60 mg/kg/day of emtricitabine (*21*).

Flow cytometric analysis and sorting of mouse hematopoietic cells

Bone marrow was flushed from one tibia and one femur using staining medium (Ca^{2+}- and Mg^{2+}-free Hank's balanced salt solution (HBSS) supplemented with 2% heat-inactivated bovine serum). Spleens were mechanically dissociated by crushing them between two glass slides. The cells were dissociated into single cell suspensions by gently passing through a 25-gauge needle and then filtering through 70-μm nylon mesh. Cells were counted, and stained with antibodies by incubating cell suspensions on ice for 30 min. For analysis of HSCs, cells were stained with fluorophore-conjugated antibodies against lineage markers (CD2, CD3, CD5, CD8a, Gr1, Ter119, and B220), as well as c-kit, Sca-1, CD150 and CD48 (see table S3 for details related to antibodies). For analysis of restricted progenitors, the cells were stained with fluorophore-conjugated antibodies against lineage markers, c-kit, Sca-1, CD16/32, CD34, CD105, and CD150. For analysis of differentiated cells, cells were stained with fluorophore-conjugated antibodies against Mac-1, Gr-1, B220, CD3, Ter119 and CD71. Cells were analyzed using a FACS Canto RUO (BD Biosciences) or a FACS Lyric (BD Biosciences) cytometer. Dead cells were identified and gated out of all analyses by including 1 μg/ml 4′,6-diamidino-2-phenylindole (DAPI) or propidium iodide in the staining medium used to resuspend cells for flow cytometry. Flow cytometry data were analyzed using Flowjo (BD Biosciences). The markers used to identify cell populations are summarized in table S2 and the flow cytometry gates are shown in figs. S1 and S2.

Competitive reconstitution assays

Recipient mice (CD45.1/CD45.2) were irradiated using an XRAD 320 x-ray irradiator (Precision X-Ray) with two doses of 540 rad delivered at least 3 hours apart. For bone marrow transplantation, 5×10^5 bone marrow cells from donor (CD45.2) mice and 5×10^5 bone marrow cells from competitor mice (CD45.1) were mixed and injected intravenously through the retro-orbital venous sinus into recipient mice (CD45.2/CD45.1). For spleen transplantation, 1.5×10^6 spleen cells from donor (CD45.2) and 3×10^5 bone marrow cells from competitor mice (CD45.1) were mixed and injected intravenously through the retro-orbital venous sinus into recipient mice (CD45.2/CD45.1). For spleen transplantation from pregnant donors, 1.5×10^6 spleen cells from the donor (CD45.2) and 5×10^5 bone marrow cells from competitor mice (CD45.1) were mixed and injected intravenously into recipient mice (CD45.2/CD45.1).

Every 4 weeks until 16 weeks after transplantation, 50 to 100 μl of blood was collected from the tail vein and mixed with 200 μl of 10 mM EDTA in PBS to prevent clotting. Cells were subjected to ammonium-chloride potassium chloride red cell lysis. Cells were stained with antibodies against CD45.1 (A20, Biolegend #110706), CD45.2 (104, Tonbo #75-0454), Mac-1 (M1/70, Thermo #47-0112-82), Gr-1 (RB6-8C5, Tonbo #60-5931), B220 (RA3-6B2, Tonbo #20-0452) and CD3 (17A2, Biolegend #100206) to evaluate the frequencies of donor Mac-1$^+$Gr-1$^+$ myeloid cells, B220$^+$ B cells, and CD3$^+$ T cells. All antibodies were used at 1:200 dilution and cells were stained for 30 min on ice.

BrdU incorporation

Mice were intraperitoneally injected with 0.1 mg/g body mass of BrdU dissolved in PBS and maintained on 1 mg/ml BrdU in the drinking water for 72 hours for HSC analysis in non-pregnant mice and 24 hours for HSCs in pregnant mice. Bone marrow cells were obtained from the spine and legs and c-kit$^+$ cells were enriched as described above. HSCs were double sorted into a 1.5 ml tube containing 2×10^6 carrier bone marrow cells from a mouse not treated with BrdU. The cells were then stained for BrdU using the BD APC BrdU Flow Kit following the manufacturer's instructions. HSCs were distinguished from unstained carrier cells based on c-kit staining. BrdU levels in HSCs were analyzed using a FACSAria II cytometer. The markers used to identify HSCs are summarized in table S2 and the flow cytometry gates are shown in figs. S1 and S2.

Immunofluorescence and confocal imaging

HSCs were double sorted into PBS and allowed to adhere to poly-L-lysine–coated cover slips (Corning) for 30 min at 4°C. Cells were then fixed with 4% paraformaldehyde for 15 min and then permeabilized in PBS-0.5% Triton X-100 for 5 min, washed 3 times with PBS, then blocked for 45 min in PBS containing 3% BSA (PBS-BSA) and incubated with primary antibody diluted in PBS-BSA for 60 min. Cells were then washed 3 times with PBS-0.05% Triton X-100 and incubated with secondary antibody in PBS-BSA for 60 min, then washed 3 times with PBS-0.05% Triton X-100. Following primary and secondary antibody incubation, cells were incubated with Dylight phalloidin (to stain F-actin; 13054S, Cell Signaling Technology, 1:200) in PBS for 15 min, then rinsed 3 times with PBS. Cells were incubated in DAPI (4ug/ml) to visualize nuclei. ProLong Gold Antifade (Fisher Scientific) was used for mounting. Images were acquired using a Nikon W1 spinning disk confocal microscope at 100x. The primary antibody was anti-phosphoSTING. Secondary antibody was goat anti-rabbit Alexa Fluor 647. For quantification of confocal immunofluorescence images, an automated macro was developed and implemented using FIJI to facilitate the analysis of the image data. A maximum intensity (MAXI) projection was generated of the Z-stack images which were obtained to cover the entire volume of the cells. Phalloidin staining was used to determine cell size/shape and to define the region of interest (ROI) for each cell. Within these ROIs, the macro calculated the total integrated density of the fluorescence signal from the protein of interest (phosphoSTING). Background fluorescence, measured in an area with no cells, was subtracted to correct for non-specific signals. The total integrated density was normalized against cell size.

Measurement of cytokines

Blood plasma was obtained after centrifugation at 900xg for 10 minutes. Bone marrow plugs and spleens were lysed in protein lysis buffer (100 mM Tris, 150 mM NaCl, 1 mM EGTA, 1 mM EDTA, 1% Triton and 0.5% sodium deoxycholate). Cytokines were measured using PBL high-sensitivity IFNα mouse ELISA kit and Biolegend LEGENDplex (Biolegend Mouse Inflammation Panel #740446) according to the manufacturer's instructions. Data were analyzed using the LEGENDplex Data Analysis Software. All samples were analyzed in duplicate.

RNA extraction and real-time qPCR from mouse hematopoietic cells

For RNA extraction from sorted hematopoietic cells, 500 to 1000 splenic HSCs or 2000 to 10,000 cells of all other cell types were double sorted into 300 μl of buffer RLT plus (Qiagen RNeasy Plus Micro kit) and purified according to the manufacturer's instructions. RNA was reverse transcribed using iScript Reverse Transcription Supermix (Bio-Rad). Transcript levels were normalized to *Actb* and fold change was calculated using the ΔCt method.

Sorting of human hematopoietic cells

Blood was collected into S-Monovette EDTA tubes from healthy pregnant females between 11 and 35 weeks of gestation with no evidence of hematopoietic malignancies. Peripheral blood mononuclear cells (PBMCs) were isolated from the samples via density gradient centrifugation (Biocoll, Bio X Cell, #BS.L6115) for 30 min at 1400 rpm at room temperature. The PBMC fraction was washed with PBS and the cells were resuspended in PBS supplemented with 10% fetal bovine serum (FBS). Total PBMC number and PBMC viability was determined for each sample. PBMCs were stained with directly conjugated antibodies against human CD3, CD4, CD8, CD14, CD235, CD56, CD34, CD38, and the viability dye SYTOX Blue (Invitrogen, S11348) for 30 min on ice. Cells were then washed and resuspended in staining medium (PBS supplemented with 5% FBS). Lineage$^-$CD34$^+$CD38$^-$ cells, which are highly enriched for HSCs, were isolated using a FACSAria III flow cytometer. The markers used to identify human Lineage$^-$CD34$^+$CD38$^-$

cells are summarized in table S2 and the flow cytometry gates are shown in fig. S12. Analysis of human samples was conducted in accordance with the local ethics committee at the West German Biobank Essen (no. 12-5212-BO). Informed consent was obtained from study participants. Samples were collected from females whose age ranged from 27 to 40 years.

RNA sequencing using human hematopoietic cells

Cells were sorted into RLT buffer (Qiagen RNeasy Mini kit), and RNA was purified according to the manufacturer's instructions. RNA quality was validated using a Pico Bioanalyzer. Libraries were generated with Watchmaker RNA Library Prep Kit (Watchmaker Genomics Limited, London, UK) using xGen Stubby Adapter-UDI Primers (IDT, Coralville, IA, USA). Libraries were quantified using the Qubit dsDNA high sensitivity-assay kit (Invitrogen, Waltham, MA, USA) and Agilent Bioanalyzer DNA chips. Libraries were sequenced using an Illumina NextSeq 2000 with 300 base pair paired-end sequencing. The quality of RNA-seq raw reads was checked using FastQC 0.11.8. Raw reads were trimmed using TrimGalore 0.6.4 and mapped to the Ensembl GRCh38 human reference genome using STAR2.7.9a. Mapped reads were quantified using TETranscripts 2.2.1. Quantified mapped reads were normalized using DESeq2 1.30.0 with R 4.0.2. Differential expression was assessed using DESeq2 1.30.0. Gene set enrichment analyses were performed using GSEA 4.1.0. Dot plots showing gene set enrichment analyses were made in R using the ggplot2 package. Heat maps showing the fold-change of deregulated genes were made in R using the ggplots2 and pheatmap packages. Retrotransposon gene sets were from TETranscripts 2.2.1 while all other gene sets were from the Molecular Signature Database (MSigDB). In Fig. 5I, the Vaccine immune response gene set was annotated as "Hoek B cell 2011 2012 tiv adult 7dy up" in MSigDB, the Adrenal erythroblast gene set was annotated as "DESCARTES adrenal erythroblasts" in MSigDB, and the Autophagy targets gene set was annotated as "Cadwell Atg16l1 targets up" in MSigDB.

Peripheral blood cell counts in humans

Blood cell counts were acquired at the University Hospital Essen by retrospectively reviewing the electronic medical records of eligible participants. We assembled a list of females ranging in age from 25 to 36 years who had routine blood draws during pregnancy over the last five years at the University Hospital Essen and then reviewed their medical histories to exclude those with a history of hematological malignancies. We identified the subset of these individuals who had routine blood draws at least one month before and two months after gestational day 1. To identify a cohort of

people that were HIV positive, pregnant and taking reverse transcriptase inhibitors, we applied the same set of criteria except that patients were additionally screened for an undetectable HIV viral load, as well as reverse transcriptase inhibitor use beginning at least one year prior to becoming pregnant. Patient records were reviewed to assess white blood cell counts, hemoglobin, platelet counts, and HIV viral load (when applicable) before and during pregnancy. A retrospective review of patient records was conducted in accordance with local ethics committee approval at the University Hospital Essen (no. 24-11998-BO). As the retrospective analyses of medical records did not require interactions or interventions with patients, and the data were shared in an anonymized manner, the Institutional Review Board waived the need to obtain signed informed consent from patients at the time of this data collection.

Statistical methods

Mice were allocated to experiments randomly and samples processed in an arbitrary order, but formal randomization techniques were not used. No formal blinding was applied when performing the experiments or analyzing the data. Sample sizes were not predetermined on the basis of statistical power calculations but were based on our experience with these assays. No data were excluded. Different replicates typically reflected samples obtained from different mice, although in competitive transplant assays the same mice were repeatedly bled at different timepoints from 4 to 16 weeks after transplantation.

Before analyzing the statistical significance of differences among groups, we tested whether data were normally distributed and whether variance was similar among groups. To test for normality, we performed Shapiro-Wilk tests when $3 \leq n < 20$ or D'Agostino Omnibus tests when $n \geq 20$. To test whether variability significantly differed among groups, we performed F-tests (for experiments with two groups) or Levene's median tests (for experiments with more than two groups). When the data significantly deviated from normality or variability significantly differed among groups, we $\log_2$ transformed the data and tested again for normality and variability. If the transformed data no longer significantly deviated from normality and equal variability, we performed parametric tests on the transformed data. If $\log_2$ transformation was not possible or the transformed data still significantly deviated from normality or equal variability, we performed non-parametric tests on the non-transformed data. The dagoTest and shapiroTest functions of the fBasics package in R were used to perform the normality tests, and the leveneTest function of the car package in R was used to perform the Levene's median test for variances.

When data or $\log_2$-transformed data were normally distributed and equally variable, sta-

tistical analyses were performed using Student's t-tests or paired t-tests (two groups), one-sample t-tests (when there was only one group), one-way ANOVAs (when there were more than two groups), two-way ANOVAs, or matched-samples two-way ANOVAs (when there were two or more groups with multiple tissues). When the data or $\log_2$-transformed data were normally distributed but unequally variable, statistical analyses were performed using Welch's t-tests (when there were two groups). When the data and $\log_2$-transformed data were abnormally distributed or unequally variable, statistical analysis was performed using Mann-Whitney tests (when there were two groups), Kruskal-Wallis tests (when there were more than two groups), Friedman tests (when there were more than two paired groups), or nparLD tests for the overall differences between transplants and Mann-Whitney tests for the differences within time points (when there were two groups measured at multiple timepoints). P values from multiple comparisons were adjusted using Sidak's method after ANOVAs or Dunn's method after Kruskal-Wallis tests or Friedman tests. Holm-Sidak's method was used to adjust comparisons involving multiple Student's t-tests, Welch's t-tests, paired t-tests, Mann-Whitney tests, or nparLD tests. All statistical tests were two-sided. All data represent mean ± standard deviation. Statistical tests were performed using GraphPad Prism V10.1.2 or R 4.0.2.

REFERENCES AND NOTES

1. D. Nakada *et al.*, Oestrogen increases haematopoietic stem-cell self-renewal in females and during pregnancy. *Nature* **505**, 555–558 (2014). doi: 10.1038/nature12932; pmid: 24451543
2. T. S. Kickler, J. L. Spivak, Effect of repeated whole blood donations on serum immunoreactive erythropoietin levels in autologous donors. *JAMA* **260**, 65–67 (1988). doi: 10.1001/jama.1988.03410010073038; pmid: 3379725
3. B. L. Ebert, H. F. Bunn, Regulation of the erythropoietin gene. *Blood* **94**, 1864–1877 (1999). doi: 10.1182/blood.V94.6.1864; pmid: 10477715
4. S. H. Cheshier, S. S. Prohaska, I. L. Weissman, The effect of bleeding on hematopoietic stem cell cycling and self-renewal. *Stem Cells Dev.* **16**, 707–718 (2007). doi: 10.1089/scd.2007.0017; pmid: 17999593
5. Y. Li *et al.*, Inflammatory signaling regulates embryonic hematopoietic stem and progenitor cell production. *Genes Dev.* **28**, 2597–2612 (2014). doi: 10.1101/gad.253302.114; pmid: 25395663
6. S. Sawamiphak, Z. Kontarakis, D. Y. Stainier, Interferon gamma signaling positively regulates hematopoietic stem cell emergence. *Dev. Cell* **31**, 640–653 (2014). doi: 10.1016/j.devcel.2014.11.007; pmid: 25490269
7. Q. He *et al.*, Inflammatory signaling regulates hematopoietic stem and progenitor cell emergence in vertebrates. *Blood* **125**, 1098–1106 (2015). doi: 10.1182/blood-2014-09-601542; pmid: 25540193
8. R. Espín-Palazón *et al.*, Proinflammatory signaling regulates hematopoietic stem cell emergence. *Cell* **159**, 1070–1085 (2014). doi: 10.1016/j.cell.2014.10.031; pmid: 25416946
9. J. T. Weinreb *et al.*, Excessive R-loops trigger an inflammatory cascade leading to increased HSPC production. *Dev. Cell* **56**, 627–640.e5 (2021). doi: 10.1016/j.devcel.2021.02.006; pmid: 33651979
10. C. Feschotte, E. J. Pritham, DNA transposons and the evolution of eukaryotic genomes. *Annu. Rev. Genet.* **41**, 331–368 (2007). doi: 10.1146/annurev.genet.40.110405.090448; pmid: 18076328
11. P. Yu *et al.*, Nucleic acid-sensing Toll-like receptors are essential for the control of endogenous retrovirus viremia and

ERV-induced tumors. *Immunity* **37**, 867–879 (2012). doi: 10.1016/j.immuni.2012.07.018; pmid: 23142781

12. S. Akira, K. Takeda, Toll-like receptor signalling. *Nat. Rev. Immunol.* **4**, 499–511 (2004). doi: 10.1038/nri1391; pmid: 15229469

13. J. Du et al., Transposable elements potentiate radiotherapy-induced cellular immune reactions via RIG-I-mediated virus-sensing pathways. *Commun. Biol.* **6**, 818 (2023). doi: 10.1038/s42003-023-05080-x; pmid: 37543704

14. S. Lefkopoulos et al., Repetitive Elements Trigger RIG-I-like Receptor Signaling that Regulates the Emergence of Hematopoietic Stem and Progenitor Cells. *Immunity* **53**, 934–951.e9 (2020). doi: 10.1016/j.immuni.2020.10.007; pmid: 33159854

15. D. Thoresen et al., The molecular mechanism of RIG-I activation and signaling. *Immunol. Rev.* **304**, 154–168 (2021). doi: 10.1111/imr.13022; pmid: 34514601

16. J. Rehwinkel, M. U. Gack, RIG-I-like receptors: Their regulation and roles in RNA sensing. *Nat. Rev. Immunol.* **20**, 537–551 (2020). doi: 10.1038/s41577-020-0288-3; pmid: 32203325

17. T. Clapes et al., Chemotherapy-induced transposable elements activate MDA5 to enhance haematopoietic regeneration. *Nat. Cell Biol.* **23**, 704–717 (2021). doi: 10.1038/s41556-021-00707-9; pmid: 34253898

18. D. Roulois et al., DNA-Demethylating Agents Target Colorectal Cancer Cells by Inducing Viral Mimicry by Endogenous Transcripts. *Cell* **162**, 961–973 (2015). doi: 10.1016/j.cell.2015.07.056; pmid: 26317465

19. L. Sun, J. Wu, F. Du, X. Chen, Z. J. Chen, Cyclic GMP-AMP synthase is a cytosolic DNA sensor that activates the type I interferon pathway. *Science* **339**, 786–791 (2013). doi: 10.1126/science.1232458; pmid: 23258413

20. D. Gao et al., Cyclic GMP-AMP synthase is an innate immune sensor of HIV and other retroviruses. *Science* **341**, 903–906 (2013). doi: 10.1126/science.1240933; pmid: 23929945

21. D. S. Lima-Junior et al., Endogenous retroviruses promote homeostatic and inflammatory responses to the microbiota. *Cell* **184**, 3794–3811.e19 (2021). doi: 10.1016/j.cell.2021.05.020; pmid: 34166614

22. H. Okude, D. Ori, T. Kawai, Signaling Through Nucleic Acid Sensors and Their Roles in Inflammatory Diseases. *Front. Immunol.* **11**, 625833 (2021). doi: 10.3389/fimmu.2020.625833; pmid: 33633744

23. D. Sun et al., Epigenomic profiling of young and aged HSCs reveals concerted changes during aging that reinforce self-renewal. *Cell Stem Cell* **14**, 673–688 (2014). doi: 10.1016/j.stem.2014.03.002; pmid: 24792119

24. V. Gorbunova et al., The role of retrotransposable elements in ageing and age-associated diseases. *Nature* **596**, 43–53 (2021). doi: 10.1038/s41586-021-03542-y; pmid: 34349292

25. D. Barbieri et al., Thrombopoietin protects hematopoietic stem cells from retrotransposon-mediated damage by promoting an antiviral response. *J. Exp. Med.* **215**, 1463–1480 (2018). doi: 10.1084/jem.20170997; pmid: 29615469

26. K. B. Chiappinelli et al., Inhibiting DNA Methylation Causes an Interferon Response in Cancer via dsRNA Including Endogenous Retroviruses. *Cell* **169**, 361 (2017). doi: 10.1016/j.cell.2017.03.036; pmid: 28388418

27. C. R. Hagan, R. F. Sheffield, C. M. Rudin, Human Alu element retrotransposition induced by genotoxic stress. *Nat. Genet.* **35**, 219–220 (2003). doi: 10.1038/ng1259; pmid: 14578886

28. H. Kobayashi et al., Bacterial c-di-GMP affects hematopoietic stem/progenitors and their niches through STING. *Cell Rep.* **11**, 71–84 (2015). doi: 10.1016/j.celrep.2015.02.066; pmid: 25843711

29. T. Clapes, S. Lefkopoulos, E. Trompouki, Stress and Non-Stress Roles of Inflammatory Signals during HSC Emergence and Maintenance. *Front. Immunol.* **7**, 487 (2016). doi: 10.3389/fimmu.2016.00487; pmid: 27872627

30. M. A. Essers et al., IFNalpha activates dormant haematopoietic stem cells in vivo. *Nature* **458**, 904–908 (2009). doi: 10.1038/nature07815; pmid: 19212321

31. M. T. Baldridge, K. Y. King, N. C. Boles, D. C. Weksberg, M. A. Goodell, Quiescent haematopoietic stem cells are activated by IFN-gamma in response to chronic infection. *Nature* **465**, 793–797 (2010). doi: 10.1038/nature09135; pmid: 20535209

32. N. Dressel et al., Activation of the cGAS/STING Axis in Genome-Damaged Hematopoietic Cells Does Not Impact Blood Cell Formation or Leukemogenesis. *Cancer Res.* **83**, 2858–2872 (2023). doi: 10.1158/0008-5472.CAN-22-3860; pmid: 37335136

33. Y. Jin, O. H. Tam, E. Paniagua, M. Hammell, TEtranscripts: A package for including transposable elements in differential expression analysis of RNA-seq datasets. *Bioinformatics* **31**, 3593–3599 (2015). doi: 10.1093/bioinformatics/btv422; pmid: 26206304

34. E. E. Swinstead et al., Steroid Receptors Reprogram FoxA1 Occupancy through Dynamic Chromatin Transitions. *Cell* **165**, 593–605 (2016). doi: 10.1016/j.cell.2016.02.067; pmid: 27062924

35. S. J. Elsässer, K. M. Noh, N. Diaz, C. D. Allis, L. A. Banaszynski, Histone H3.3 is required for endogenous retroviral element silencing in embryonic stem cells. *Nature* **522**, 240–244 (2015). doi: 10.1038/nature14345; pmid: 25938714

36. G. Kassiotis, J. P. Stoye, Immune responses to endogenous retroelements: Taking the bad with the good. *Nat. Rev. Immunol.* **16**, 207–219 (2016). doi: 10.1038/nri.2016.27; pmid: 27026073

37. K. H. Mayer et al., Emtricitabine and tenofovir alafenamide vs emtricitabine and tenofovir disoproxil fumarate for HIV pre-exposure prophylaxis (DISCOVER): Primary results from a randomised, double-blind, multicentre, active-controlled, phase 3, non-inferiority trial. *Lancet* **396**, 239–254 (2020). doi: 10.1016/S0140-6736(20)31065-5; pmid: 32711800

38. G. Banuelos-Sanchez et al., Synthesis and Characterization of Specific Reverse Transcriptase Inhibitors for Mammalian LINE-1 Retrotransposons. *Cell Chem. Biol.* **26**, 1095–1109.e14 (2019). doi: 10.1016/j.chembiol.2019.04.010; pmid: 31155508

39. C. Zhang et al., Structural basis of STING binding with and phosphorylation by TBK1. *Nature* **567**, 394–398 (2019). doi: 10.1038/s41586-019-1000-2; pmid: 30842653

40. J. D. Sauer et al., The N-ethyl-N-nitrosourea-induced Goldenticket mouse mutant reveals an essential function of Sting in the in vivo interferon response to Listeria monocytogenes and cyclic dinucleotides. *Infect. Immun.* **79**, 688–694 (2011). doi: 10.1128/IAI.00999-10; pmid: 21098106

41. X. Zhang, X. C. Bai, Z. J. Chen, Structures and Mechanisms in the cGAS-STING Innate Immunity Pathway. *Immunity* **53**, 43–53 (2020). doi: 10.1016/j.immuni.2020.05.013; pmid: 32668227

42. X. Zhang et al., The cytosolic DNA sensor cGAS forms an oligomeric complex with DNA and undergoes switch-like conformational changes in the activation loop. *Cell Rep.* **6**, 421–430 (2014). doi: 10.1016/j.celrep.2014.01.003; pmid: 24462292

43. T. Sato et al., Interferon regulatory factor-2 protects quiescent hematopoietic stem cells from type I interferon-dependent exhaustion. *Nat. Med.* **15**, 696–700 (2009). doi: 10.1038/nm.1973; pmid: 19483695

44. W. M. Schneider, M. D. Chevillotte, C. M. Rice, Interferon-stimulated genes: A complex web of host defenses. *Annu. Rev. Immunol.* **32**, 513–545 (2014). doi: 10.1146/annurev-immunol-032713-120231; pmid: 24555472

45. R. Kamada et al., Interferon stimulation creates chromatin marks and establishes transcriptional memory. *Proc. Natl. Acad. Sci. U.S.A.* **115**, E9162–E9171 (2018). doi: 10.1073/pnas.1720930115; pmid: 30201712

46. J. Ahn, S. Son, S. C. Oliveira, G. N. Barber, STING-Dependent Signaling Underlies IL-10 Controlled Inflammatory Colitis. *Cell Rep.* **21**, 3873–3884 (2017). doi: 10.1016/j.celrep.2017.11.101; pmid: 29281834

47. U. Müller et al., Functional role of type I and type II interferons in antiviral defense. *Science* **264**, 1918–1921 (1994). doi: 10.1126/science.8009221; pmid: 8009221

48. I. Cañadas et al., Tumor innate immunity primed by specific interferon-stimulated endogenous retroviruses. *Nat. Med.* **24**, 1143–1150 (2018). doi: 10.1038/s41591-018-0116-5; pmid: 30038220

49. L. W. Terstappen, S. Huang, M. Safford, P. M. Lansdorp, M. R. Loken, Sequential generations of hematopoietic colonies derived from single nonlineage-committed CD34+CD38− progenitor cells. *Blood* **77**, 1218–1227 (1991). doi: 10.1182/blood.V77.6.1218.1218; pmid: 1705833

50. D. C. Hancks, H. H. Kazazian Jr., Active human retrotransposons: Variation and disease. *Curr. Opin. Genet. Dev.* **22**, 191–203 (2012). doi: 10.1016/j.gde.2012.02.006; pmid: 22406018

51. K. L. Hoek et al., A cell-based systems biology assessment of human blood to monitor immune responses after influenza vaccination. *PLOS ONE* **10**, e0118528 (2015). doi: 10.1371/journal.pone.0118528; pmid: 25706537

52. J. Cao et al., A human cell atlas of fetal gene expression. *Science* **370**, eaba7721 (2020). doi: 10.1126/science.aba7721; pmid: 33184181

53. R. W. Eisinger, C. W. Dieffenbach, A. S. Fauci, HIV Viral Load and Transmissibility of HIV Infection: Undetectable Equals Untransmittable. *JAMA* **321**, 451–452 (2019). doi: 10.1001/jama.2018.21167; pmid: 30629090

54. P. A. Tovo et al., Pregnancy Is Associated with Impaired Transcription of Human Endogenous Retroviruses and of TRIM28 and SETDB1, Particularly in Mothers Affected by Multiple Sclerosis. *Viruses* **15**, 710 (2023). doi: 10.3390/v15030710; pmid: 36992419

55. R. Cordaux, M. A. Batzer, The impact of retrotransposons on human genome evolution. *Nat. Rev. Genet.* **10**, 691–703 (2009). doi: 10.1038/nrg2640; pmid: 19763152

56. J. Wu, N. Dobbs, K. Yang, N. Yan, Interferon-Independent Activities of Mammalian STING Mediate Antiviral Response and Tumor Immune Evasion. *Immunity* **53**, 115–126.e5 (2020). doi: 10.1016/j.immuni.2020.06.009; pmid: 32640258

57. S. Cerboni et al., Intrinsic antiproliferative activity of the innate sensor STING in T lymphocytes. *J. Exp. Med.* **214**, 1769–1785 (2017). doi: 10.1084/jem.20161674; pmid: 28484079

58. X. Gui et al., Autophagy induction via STING trafficking is a primordial function of the cGAS pathway. *Nature* **567**, 262–266 (2019). doi: 10.1038/s41586-019-1006-9; pmid: 30842662

59. D. L. Jacobson et al., Maternal anemia and preterm birth among women living with HIV in the United States. *Am. J. Clin. Nutr.* **113**, 1402–1410 (2021). doi: 10.1093/ajcn/nqaa441; pmid: 35104854

60. F. Masaisa, J. B. Gahutu, J. Mukiibi, J. Delanghe, J. Philippé, Anemia in human immunodeficiency virus-infected and uninfected women in Rwanda. *Am. J. Trop. Med. Hyg.* **84**, 456–460 (2011). doi: 10.4269/ajtmh.2011.10-0519; pmid: 21363986

61. J. de Boer et al., Transgenic mice with hematopoietic and lymphoid specific expression of Cre. *Eur. J. Immunol.* **33**, 314–325 (2003). doi: 10.1002/immu.200310005; pmid: 12548562

62. J. R. Prigge et al., Type I IFNs Act upon Hematopoietic Progenitors To Protect and Maintain Hematopoiesis during Pneumocystis Lung Infection in Mice. *J. Immunol.* **195**, 5347–5357 (2015). doi: 10.4049/jimmunol.1501553; pmid: 26519535

63. T. Hulsen, DeepVenn - a web application for the creation of area-proportional Venn diagrams using the deep learning framework Tensorflow. arXiv:2210.04597 [cs.HC] (2022).

64. I. Rusinova et al., Interferome v2.0: An updated database of annotated interferon-regulated genes. *Nucleic Acids Res.* **41** (D1), D1040–D1046 (2013). doi: 10.1093/nar/gks1215; pmid: 23203888

65. F. C. Grandi, H. Modi, L. Kampman, M. R. Corces, Chromatin accessibility profiling by ATAC-seq. *Nat. Protoc.* **17**, 1518–1552 (2022). doi: 10.1038/s41596-022-00692-9; pmid: 35478247

SUPPLEMENTARY MATERIALS

science.org/doi/10.1126/science.ado6836
Figs. S1 to S12
Tables S1 to S4
References (66–69)